國立臺灣大學醫學院暨工學院醫學工程學研究所

碩士論文

Department of Biomedical Engineering
College of Medicine and College of Engineering
National Taiwan University

Master's Thesis

血管平滑肌細胞對於延長培養與物理刺激的表現反應

Vascular Smooth Muscle Cell Phenotypic Responses to Prolonged Subculture and Physical Stimulation

薛煜煜

Yu-Yu Hsueh

指導教授：趙本秀博士

Advisor: Pen-Hsiu Grace Chao, Ph.D.

中華民國 113 年 9 月

September, 2024

doi:10.6342/NTU202403815

摘要

心血管疾病是全球主要死因，其中血管老化扮演關鍵角色。血管平滑肌細胞的表現型調控在疾病與老化的進程當中至關重要。本研究透過長期培養和早衰素(progerin)表達及物理刺激探討細胞老化和機械訊號對血管平滑肌細胞表型變化的影響。早衰素源自早年衰老症候群，會加速病人老化。使用直線纖維和捲曲纖維的靜電紡絲支架模擬老化/病理與健康/年輕的動脈結構。經過長期繼代和衰老素表達模擬老化顯著降低了初代培養血管平滑肌細胞的表現收縮標記（α-SMA、SM-22、Calponin-1）並增加細胞增殖，特別是在直纖維上。即使在晚期代數和衰老素表達的細胞中，捲曲纖維也部分促進細胞保持收縮表型。機械拉伸揭示了複雜的基因表達反應。收縮基因（*Acta2*、*Taglin*、*Cnn1*、*Myh11*）和合成基因（*Spp1*、*Klf5*、*Col1a1*）受細胞繼代、早衰素表達、支架結構與機械拉伸的差異調控。本研究提供了血管老化機制的洞見，並提供了一個研究血管平滑肌細胞表現型的平台，對於心血管疾病的組織工程和治療策略具有潛在應用。

關鍵詞：血管平滑肌細胞、表現型調控、早衰素、機械刺激、靜電紡絲、心血管老化、組織工程。

doi:10.6342/NTU202403815

Abstract

Cardiovascular diseases (CVDs) are the leading cause of death globally, where aging plays a crucial role. The phenotypic modulation of vascular smooth muscle cells (VSMCs) is a key factor in the disease and aging process. This study investigates the effects of cellular aging and mechanical cues on VSMC phenotypic changes through prolonged culture, progerin expression, and physical stimulation. Progerin, associated with Hutchinson-Gilford progeria syndrome (HGPS), induces accelerated aging in patients. Electrospun scaffolds with straight and crimped fibers mimicked aged/pathological and healthy/young arterial structures, respectively. Simulated aging by prolonged passaging and progerin expression significantly decreased contractile marker expression (α-SMA, SM-22, Calponin-1) and increased proliferation in primary VSMCs, especially on straight fibers. Crimped fibers partially preserved the contractile phenotype even in later passages and progerin-expressing cells. Mechanical loading revealed complex gene expression responses. Contractile (*Acta2, Taglin, Cnn1, Myh11*) and synthetic genes (*Spp1, Klf5, Col1a1*) were differentially regulated by cell passage, progerin expression, scaffold structure and mechanical loading. This study provides insights into vascular aging mechanisms and offers a platform for studying VSMC behavior, with potential applications in tissue engineering and therapeutic strategies for CVDs.

Keywords: Vascular smooth muscle cells, VSMC, phenotypic modulation, progerin, mechanical stimulation, electrospun scaffolds, cardiovascular aging, tissue engineering.

doi:10.6342/NTU202403815

Abbreviations

CVD	Cardiovascular disease
EC	Endothelial cell
ECM	Extracellular matrix
FBS	Fetal Bovine Serum
HGPS	Hutchinson-Gilford progeria syndrome
PLA	Polylactic acid
PDMS	Polydimethylsiloxane
VSMC	Vascular smooth muscle cell

Contents

doi:10.6342/NTU202403815

doi:10.6342/NTU202403815

Figure list

doi:10.6342/NTU202403815

Table list

doi:10.6342/NTU202403815

1. Introduction

1.1. Cardiovascular diseases and aging

Cardiovascular diseases (CVDs) represent the foremost cause of global mortality, contributing to an estimated 17.9 million annual deaths, which constitutes 32% of total mortalities [1]. CVDs refer to a broad category of disorders that impact the heart and blood vessels. Notably, over 80% of CVD deaths are due to heart attacks and strokes, and a third of these tragically occur prematurely in people under 70 years old [1]. Aging is a significant factor contributing to the burden of CVDs and other age-related conditions. Over the next three decades, the global demographic of individuals aged 65 years or older is anticipated to double, reaching 1.6 billion by 2050. This demographic shift will result in older people constituting more than 16% of the global population.

CVDs encompass a range of conditions, including coronary heart disease, cerebrovascular disease, and various other related disorders., are primarily triggered by artery-related disorders such as atherosclerosis, aneurysms, atrial fibrillation, hypertension, and cardiac hypertrophy [2]. Despite the development of clinical treatments to alleviate the symptoms of these arterial abnormalities, the underlying pathologies remain incompletely understood.

Age serves as an independent risk factor for CVD in adults, with this risk further compounded by additional factors such as frailty, obesity, and diabetes [2]. As the global population ages and the prevalence of these contributing factors increases, understanding the complex pathologies of these arterial abnormalities becomes crucial in developing effective preventive and therapeutic strategies for CVDs.

doi:10.6342/NTU202403815

1.2. Arterial anatomy and function

The anatomy and function of arteries can be understood by examining the three layers and the cells within each layer. The innermost layer is called the tunica intima and is composed of endothelial cells. This layer acts as a barrier between the blood and the surrounding tissue and regulates the vascular tone and permeability [3, 4].

Vascular smooth muscle cells in the media play a crucial role in regulating vessel diameter and blood flow by contracting and relaxing. VSMCs are also involved in secreting and maintaining the ECM structure and composition of blood vessels, including collagen and elastin. Elastin fibers within the ECM confer elasticity, enabling arteries to stretch during systole and recoil during diastole. This dynamic interaction between VSMCs and the ECM ensures proper vessel function and adaptability to changing hemodynamic conditions [5, 6].

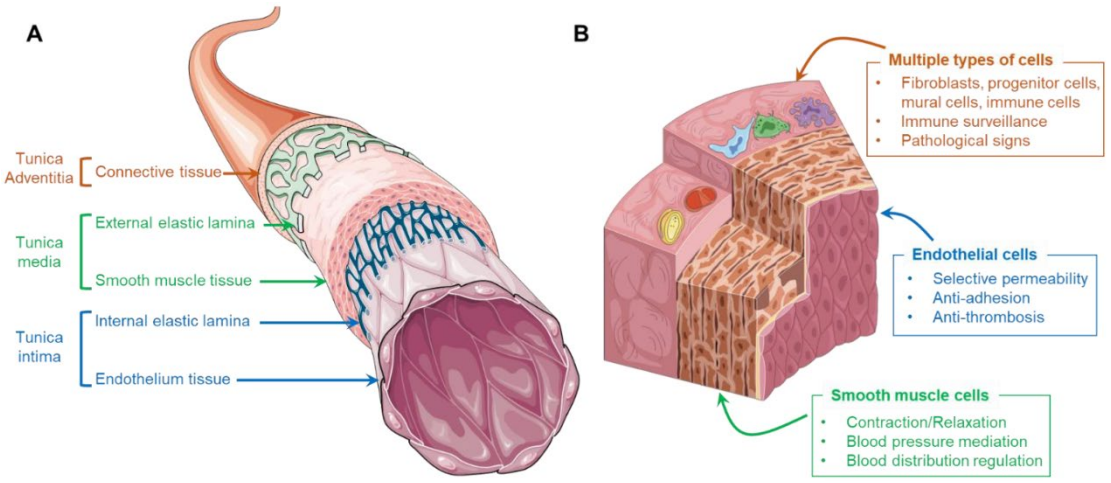

Figure 1 Arterial anatomy and composition of cells within each layers.
(A) Illustration depicting the anatomy of an artery. From outermost to innermost layers: Adventitia, Media, and Intima. (B) Highlighting the cellular composition within each layer. This figure was prepared using a template on the Sevier medical art website (https://smart.servier.com/, accessed on 12 July 2023).

doi:10.6342/NTU202403815

The outermost layer, known as the tunica adventitia, is composed of fibroblasts, collagen and connective tissue. It offers structural support to the blood vessel and produces vasoactive factors [7].

Arteries demonstrate a critical physiological property known as compliance, defined as their capacity to stretch and recoil. This inherent ability enables arteries to accommodate fluctuations in blood volume and plays a pivotal role in maintaining consistent blood pressure levels [8]. Compliance allows arteries to expand in response to increased blood flow, thereby reducing resistance and ensuring efficient circulation. Conversely, during decreased blood flow, arteries recoil to maintain pressure and continue directing blood flow to vital organs. This property of compliance is essential for the cardiovascular system's dynamic adaptation to varying physiological demands.

Vessel compliance is primarily determined by the structural composition of the arterial walls, particularly the presence and arrangement of elastin and collagen fibers. Elastin provides elasticity to the arteries, allowing them to stretch during systole and recoil during diastole, thereby maintaining blood pressure and flow [9]. Collagen, on the other hand, provides structural support and helps prevent overexpansion of the arterial walls [10]. In addition to elastin and collagen, other factors such as smooth muscle tone, endothelial function, and the composition of the extracellular matrix also influence vessel compliance.

The unique composite structure of elastin and collagen, with elastin fibers arranged in a wavy or crimped pattern intertwined with collagen fibers, contributes to the overall compliance of the vessel. This wavy arrangement allows the arterial walls to stretch and recoil in response to changes in blood pressure, ensuring efficient blood circulation and reducing the workload on the heart.

doi:10.6342/NTU202403815

1.3. Arterial section in aging and diseases

The physiology and microstructure of the artery are intimately linked to its hemodynamic environment. In pathological conditions such as aging, hypertension, inflammation, and Marfan syndrome, the microstructures of connective tissues tend to exhibit a more linear arrangement compared with the healthy arterial microstructure [10-12]. In aging arteries, for instance, there is a notable increase in collagen cross-linking and degradation of elastin within the ECM. This results in heightened ECM stiffness, compromising arterial compliance and distensibility. VSMCs undergo phenotypic changes with age. These changes include increased proliferation, migration, and production of ECM components [13, 14]. Moreover, aging VSMCs exhibit reduced contractility and altered responsiveness to vasoactive stimuli, contributing to arterial stiffening and impaired vasorelaxation [15].

Endothelial dysfunction further characterizes aging arteries, presenting with decreased nitric oxide bioavailability, escalated oxidative stress, and amplified inflammatory responses [16]. These endothelial alterations promote vasoconstriction, platelet aggregation, and leukocyte adhesion, thereby exacerbating arterial stiffness and atherosclerosis progression [17, 18].

In older mice, the aortic elastin lamina appears flattened, fragmented and disarrayed compared to younger counterparts [19]. Also, elastin content decreases with age while collagen content increases, leading to a higher collagen/elastin ratio in older animals [20-22]. Our investigation involved a comparison of aortic cross-sections between 10-week-old and 84-week-old mice. In **Figure 2**, we observed that the elastin lamina, which typically exhibits a wavy structure in younger aortas, becomes flattened in older mice.

doi:10.6342/NTU202403815

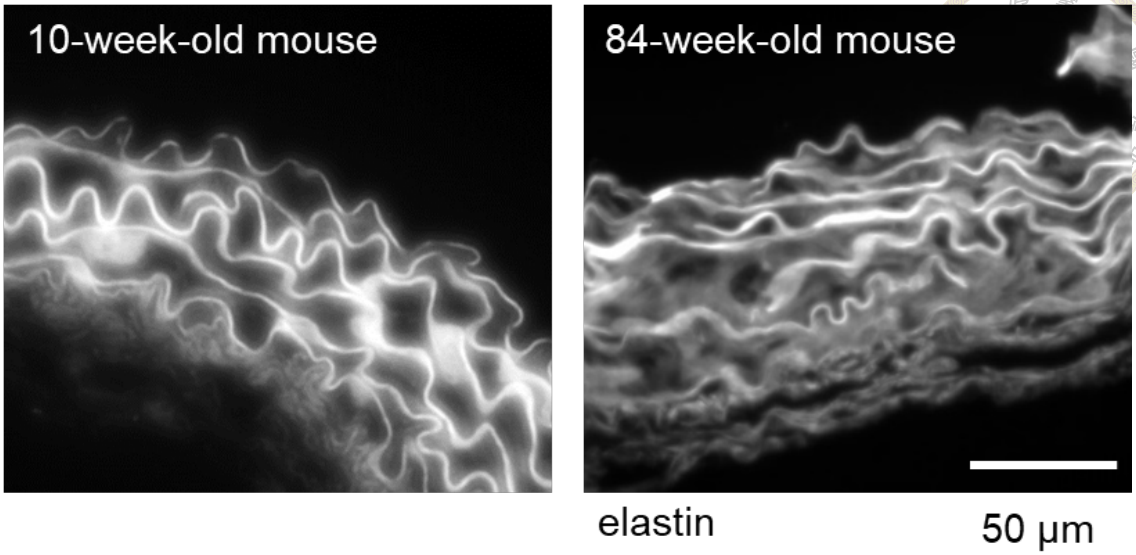

Figure 2 Cross section of young and aged mouse aorta.
The comparison of aortic cross-sections between 10-week-old and 84-week-old mice revealed notable differences in the structural integrity and composition of the tissue. Scale bar is 50 μm, Elastin was excited 488 nm and emitted autofluorescence at 525 nm.

1.4. Vascular Smooth Muscle Cells (VSMCs)

Vascular smooth muscle cells (VSMCs) are stromal cells within the vascular wall that regulate arterial tone, blood pressure, and tissue blood supply. VSMCs exhibit functional and phenotypic diversity, which varies with their location in the arterial tree, embryologic origin, and organ-dependent microenvironment [23]. VSMCs exhibit various phenotypes, but they are primarily categorized into two main types: contractile VSMCs, responsible for regulating vessel diameter, and synthetic VSMCs, involved in tissue repair and remodeling. [24].

Analyzing the gene expression of *Acta2*, *Taglin*, *Cnn1*, and *Myh11* in VSMCs is crucial as these genes are key markers of the contractile phenotype, and their expression levels reflect the functional state of VSMCs, with high expression indicating a contractile phenotype that is essential for vascular tone regulation [24]. Changes in the expression of these genes are associated with phenotypic switching of VSMCs, which contributes to

doi:10.6342/NTU202403815

vascular remodeling and disease progression.

Numerous studies have highlighted the significance of VSMCs in cardiovascular diseases, including atherosclerosis [25], aneurysms [26], hypertension [27], and thrombosis [28]. In cardiovascular aging and pathogenesis, apart from the observed changes in ECM structure, the cells within these structures also change their phenotype [9]. VSMCs exhibit remarkable cellular plasticity, where they can change phenotype in response to various stimuli. VSMCs can de-differentiate from a contractile phenotype to synthetic phenotype. The synthetic VSMCs can further differentiate into alternative phenotypes such as macrophage-like, mesenchymal-like, fibroblast-like and osteogenic VSMCs. [12, 29, 30]. The various factors changing phenotype of VSMC include cytokines, microRNAs, matrix metalloproteinases, integrins, oxidative stress, autophagy, mechanical stimulations like hemodynamic pressure and matrix stiffness, and mitochondrial metabolism alterations [31-35].

1.5. Hutchinson-Gilford progeria syndrome (HGPS)

Hutchinson-Gilford progeria syndrome (HGPS) is an accelerated-aging syndrome, caused by expression of the mutated Lamin protein, progerin [9, 10]. Progerin accumulation in VSMCs leads to altered phenotypic changes in mouse models [26, 36, 37] and humans [38]. Children with HGPS exhibit early-onset cardiovascular disease, including atherosclerosis, myocardial infarction, and stroke, leading to premature death [25]. Histological analysis of cardiovascular tissues from HGPS patients has revealed features commonly associated with aging-related cardiovascular disease, such as atherosclerosis, arteriolosclerosis and extensive fibrosis including interstitial myocardial and perivascular fibrosis [39, 40].

The presence of progerin, the mutated protein responsible for HGPS, has been

doi:10.6342/NTU202403815

detected in both HGPS and non-HGPS populations, suggesting progerin may contribute to cardiovascular aging in the normal individuals [41, 42]. Understanding the mechanisms underlying cardiovascular pathology in HGPS may provide insights into age-related cardiovascular diseases and potential therapeutic strategies.

1.6. Mechanical cues and forces

VSMCs respond to mechanical cues and forces by phenotypic changes. These cues encompass cell alignment, cell-cell interactions, substrate stiffness, and the type of extracellular matrix [11, 12, 43]. Mechanical forces acting on VSMCs include fluid shear stress, cyclic stretch, and hydrostatic pressure [34, 44]. For instance, changes in the mechanical environment, such as stretch and matrix stiffness, can prompt VSMCs to adopt a proliferative and synthetic phenotype. Additionally, VSMCs exhibit durotaxis, preferentially migrating from soft to stiffer substrates [45].

Aging causes harmful changes in the vascular system's structure and function at both the tissue and cellular levels, which significantly reduces its mechanical properties [46]. The aging process compromises the natural adaptability of the arterial wall to constantly changing mechanical forces exerted by blood flow [47-50]. This loss of adaptability is closely linked to the mechanosensation of VSMCs [43, 51-53].

Maintaining healthy VSMC mechanosensation, the ability to sense and transduce mechanical forces into intracellular signals, is essential for vessel function. Stiffening of VSMCs and dysfunctions in mechanosensation often signify the development of cardiovascular diseases [54, 55]. Thus, the decline in vessel’s compliance observed with aging can be partly attributed to impaired VSMC behavior and function.

1.7. Aim of study

This study aims to investigate how pathological/aged VSMCs react to extrinsic

doi:10.6342/NTU202403815

factors, using intrinsic aging models induced by progerin expression or extended culture. We hypothesize that crimped fibers can enhance the contractile phenotype in VSMCs with prolonged passage or progerin expression, and mechanical stretching can synergistically amplify this enhancement. Our objectives include generating straight and wavy fibrous scaffolds to recreate either healthy/young or pathological/aged arterial structures, characterizing VSMC phenotypes under these conditions, and applying mechanical stretching to discern the combined effects on VSMC phenotype.

doi:10.6342/NTU202403815

2. Material and methods

2.1. Cell resource and culture

Progerin transgenic mouse

We obtained Progerin transgenic mice through collaboration with Professor Ya-Hui Chi's laboratory at National Health Research Institutes. The comprehensive procedure for introducing human progerin (Lamin A, G608G) into the *Gt(ROSA)26Sor* site was described in [56]. To ensure ethical and high-quality research, our mice breeding protocols adhere to the guidelines set forth by the National Health Research Institutes Laboratory Animal Center in Taiwan.

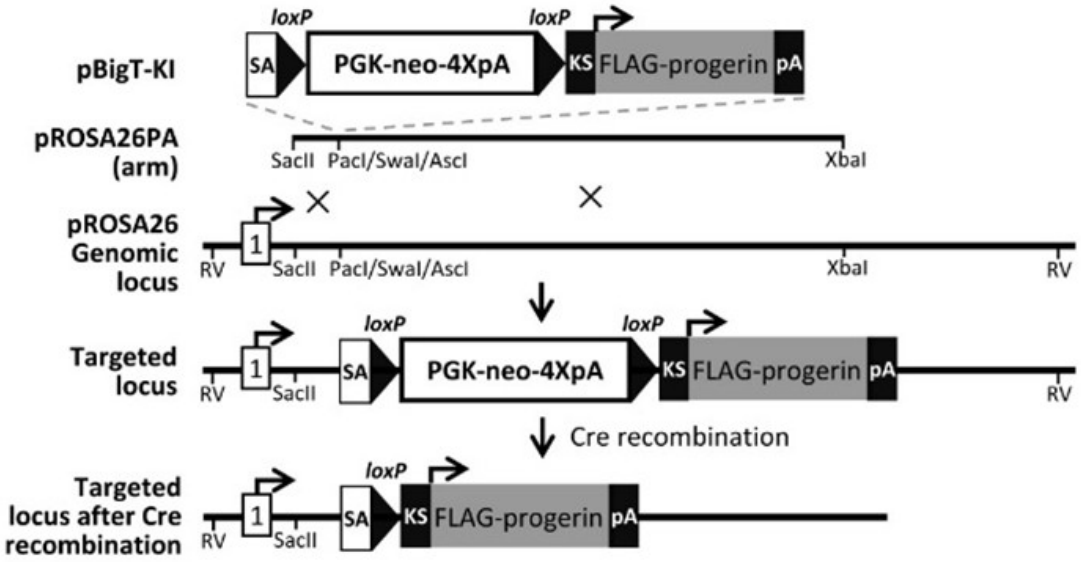

Figure 3 The genetic circuit design for the targeting vector and the targeted ROSA26 locus.

The targeting vector harbors FLAG-progerin along with a PGK-neo-4XpA cassette for antibiotic selection. Upon the expression of Cre recombinase, the PGK-neo-4XpA cassette is excised. (Figure from [56])

doi:10.6342/NTU202403815

Mouse aortic isolation

When mice reached 8-10 weeks of age, they were euthanized via carbon dioxide asphyxiation. Following euthanasia, the mice were positioned supine on a dissecting board, and the initial gross dissection was performed. All stainless-steel instruments were sterilized by moist heat, while non-sterilizable equipment was disinfected with sodium hypochlorite solution and alcohol.

The mice were then transferred to a dissecting microscope for precise manipulation. A midline thoracotomy was performed. Using sterile surgical forceps and dissecting scissors, the ribs and visceral organs were carefully removed to expose the heart and thoracic aorta. Prior to excision, the thoracic aorta was perfused with approximately 2.5-5 ml of cold PBS containing 1% antibiotic-antimycotic solution (Invitrogen, 15240062) via injection into the left ventricle to clear residual blood.

Subsequently, using micro-dissecting scissors and fine-tipped forceps, the surrounding fat and connective tissues were meticulously cleared from the thoracic aorta. The descending thoracic aorta, specifically the segment located inferior to the aortic arch and superior to the diaphragm, was then carefully isolated and excised. This excised segment was prepared for subsequent tissue explant culture.

Tissue explant culture

The isolated thoracic aorta segment was immediately transferred to a dish containing sterile PBS containing 1% antibiotic-antimycotic solution (Invitrogen, 15240062) for a subsequent cleaning process, which was visualized using a dissecting microscope. Following this, the cleaned aorta was incised along its longitudinal axis, and the intimal layer was carefully abraded with fine-tipped tweezers to remove endothelial cells.

doi:10.6342/NTU202403815

For the explant culture setup, the prepared aorta segment was then finely sectioned into small pieces. These fragments were uniformly distributed into four individual 20 µl droplets of Dulbecco's Modified Eagle Medium: Nutrient Mixture F-12 (DMEM/F-12) supplemented with 20% fetal bovine serum (Gibco, 10437-028), 1% antibiotic-antimycotic solution (Invitrogen, 15240062), and 1% GlutaMAX™ (Gibco, 35050061), strategically placed on a fresh 6 cm tissue culture dish. To ensure the aortic pieces remained submerged and adhered, individual coverslips were gently positioned over each droplet. The culture dish was then filled with an additional 5 ml of media before being carefully transferred to an incubator. Following an 18- to 21-day incubation period, primary VSMCs proliferated and migrated outwards from the aortic fragments, achieving confluence without the necessity of medium replacement. Importantly, this process concluded within the 21-day maximum incubation limit.

Cell subculture and maintain

The first passage of mouse VSMCs was performed after trypsinizing cells from coverslips. Subsequently, the VSMCs were cultured in Falcon® Cell Culture Dishes in Dulbecco's Modified Eagle Medium: Nutrient Mixture F-12 (DMEM/F-12, ThermoFisher, 11320033) supplemented with 10% fetal bovine serum (Gibco, 10437-028), 1% antibiotic-antimycotic solution (Invitrogen, 15240062), and 1% GlutaMAX™ (Gibco, 35050061). The cell seeding density was maintained at 600 cells/cm^2. The cells were passaged when approximately 90% confluent and was maintained at 37°C in a 5% CO_2 incubator.

Inducible progerin expression system

P1 VSMCs were initially seeded at a density of 600 cells/cm² in a culture dish and

doi:10.6342/NTU202403815

allowed to grow until reaching 75-80% confluency. 4-hydroxytamoxifen (4-OHT, Abcam, ab141943, dissolved in DMSO at a stock concentration of 2 mM. It was added to the culture medium at final working concentration of 1 μM.) was applied to induce the expression of Cre recombinase. This induced cassette excision resulted in the removal of the stop codon and the expression of progerin. After 72-hour treatment, the medium containing 4-OHT was replaced with fresh medium to continue the culture.

2.2. Artificial scaffold

Electrospinning

A solution of 6% w/v Poly-lactic acid (PLA, Green Square Materials Co., Ltd.) in hexafluoropropylene was electrospun at a flow rate of 3.0 ml/h, using an applied voltage of 7.1 kV and a gap distance of 16.5 cm. Simultaneously, a polyethylene oxide (PEO, Sigma #181986) solution with a concentration of 15% w/v in 90% ethanol was electrospun at a flow rate of 0.79 ml/h, applying a voltage of 6.7 kV and maintaining a gap distance of 11 cm. Utilizing opposing nozzles, two polymeric materials were extruded and subsequently collected on a rotating mandrel operating at 1350 rpm and -3 kV. This process yielded an aligned composite scaffold, characterized by PLA to PEO weight ratio of 7:3. To effectively collect fibers on the collector, a pair of restricting electrical fields with a voltage of 4 kV was applied to the top and bottom of the rotating collector.

Manufacture of microstructure on scaffold

The as-spun scaffold initially possesses a straight structure. To prepare these scaffolds, the composite structures undergo a half-hour process in tap water to eliminate the sacrificial PEO fibers and PLA fiber remains.

doi:10.6342/NTU202403815

To fabricate straight scaffolds, the PLA fiber was first rinsed for 30 minutes. It was then washed twice with tap water for 15 minutes per wash, followed by air drying overnight. Subsequently, scaffolds were positioned between two layers of glass and heated to 45℃ for half an hour.

In contrast, to create wavy scaffolds, the PLA fiber was rinsed in tap water for half an hour, then in 75% ethanol for half an hour, followed by two 15-minute washes in tap water. After air drying overnight, the scaffolds were placed between two frosted glass plates and heated on a hot plate at 85℃ for 15 minutes to induce fiber waviness.

Structure and property characterization

To analyze the fiber structure, air-dried scaffolds were imaged at 1000x magnification using a scanning electron microscope (SEM, Hitachi TM3000). Fiber crimpness was quantified from scanning electron microscopy (SEM) images using the Neuron J plugin within ImageJ, by tracing the trajectory of individual fibers. Crimpness was defined as:

$$Crimpness = \frac{L_f - L_0}{L_0}$$

$$= \frac{Real\ length\ between\ endpoints - Linear\ distance\ between\ endpoints}{Linear\ distance\ between\ endpoints}$$

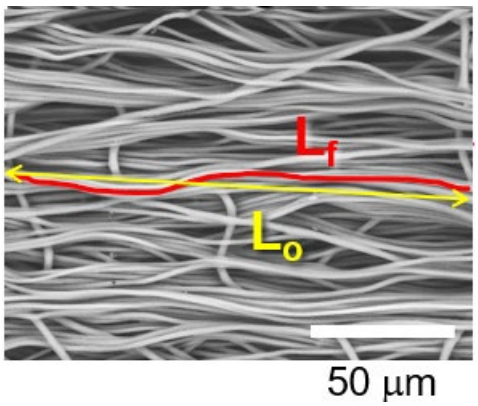

doi:10.6342/NTU202403815

The acceptable crimpness for crimped fibers should exceed 2%, whereas straight fibers should maintain a crimpness below 2%. For the experiments conducted in this study, only scaffolds exhibiting a crimpness greater than 3% were selected to ensure consistency.

The scaffold's thickness (1x4 cm^2) was measured using a laser optical sensor (Micro-Epsilon ILD 1420). To determine the average thickness of the scaffold, twenty distinct points at the center of each scaffold were sampled and measured.

The scaffolds used for this study had a measured thickness of 0.20798 ± 0.02252 mm for crimped fibers and 0.1055 ± 0.01858 mm for straight fibers. These values fall within our laboratory's typical manufacturing ranges of 0.20-0.25 mm and 0.095-0.15 mm, respectively. Uniaxial tensile tests were conducted using the BOSE ElectroForce 5500. These tests utilized a 10kg load cell and a strain rate of 0.02 mm/sec.

Scaffold sterilization and coating

The large electrospun sheets were trimmed to 1x2 cm^2 or 1x4 cm^2. These cuts were executed along the long axis to ensure a parallel alignment with the fibers. To sterilize, the scaffolds were first soaked in 75% ethanol for 30 seconds and then immersed in 35% hydrogen peroxide for an hour. After undergoing sterilization, the scaffolds were coated with a solution of dopamine hydrochloride in Trisma base (2 mg/ml, pH 8.5) for 15 minutes. Subsequently, the scaffolds were placed in a 1% solution of type 1 collagen (90 μg/ml, sourced from mouse tails, BD #354249) in PBS and incubated at 37°C overnight.

Cell culture on fibrous scaffold

To seed cells onto the fibrous scaffolds, each 1x2 cm^2 region was treated with 80 μl of cell suspension, containing 15,000 VSMCs/cm^2. The cells were allowed to attach for one hour. Following this, the fiber was flipped, and another 30,000 cells were seeded on

doi:10.6342/NTU202403815

the other side and allowed to attach for another hour. Each scaffold was then transferred into a PDMS-coated 12-well plate containing 1.5 ml of medium for long-term culture.

2.3. Assay

Cell viability

To prepare the scaffolds for cell viability assay, each scaffold (1x2 cm^2) was placed in a well of a 12-well plate, which had been coated with PDMS. On the day of the experiment, 10% of AlamarBlue dye (Invitrogen #DAL1100) was premixed with the 1 ml medium in each well and incubated at 37°C for another 3 hours. Then, 100μl of the medium from each well was transferred to a microplate, and the fluorescence intensity was measured by a plate reader (Synergy HTX, BioTek) with an excitation wavelength of 530 nm and an emission wavelength of 590 nm. The fluorescence signal was blanking to the 10% AlamarBlue in medium control without cells and normalized to the signal after 2-day culture. The scaffolds were rinsed with PBS after the AlamarBlue assay and maintained in fresh medium for further experiments.

Immunocytochemistry

The cells were fixed using 4% formaldehyde (Macron Fine Chemicals) in PBS at 37°C for 10 minutes and then washed three times, for 10 minutes each. The fixed sample can be preserved in PBS at 4°C for up to two weeks. On the day prior to imaging, the samples were permeabilized using 0.5% (v/v) Triton X-100 (Merck, #T8787) in PBS at room temperature for 20 minutes. Subsequently, the cells underwent blocking with 1% (w/v) BSA (Urinogen, UR-BSA001-100G) in PBS at room temperature for one hour. The next stage included incubation with primary antibodies, α-SMA, SM22, Calponin-1, and

doi:10.6342/NTU202403815

Progerin (FLAG-tagged), diluted (see **Table 2 Antibody**) in 1% BSA, at room temperature for one hour. Following this, the cells were treated with secondary antibodies diluted in 1% BSA and concurrently stained with DAPI (5μg/ml, Sigma #D8417) and Alexa Fluor 568 phalloidin (1:200 in 1% BSA, Invitrogen #A12380) at room temperature for an hour. Finally, the cells were mounted using Fluoromount aqueous mounting medium (Sigma #F4680) between a coverslip and slide for observation.

Microscopy

Fluorescent images of plated cells were captured using a Nikon Eclipse Ti2 E inverted widefield microscope, outfitted with a CCD camera from Hamamatsu and 20X/NA0.45 air objectives. Confocal images of cells on fibrous scaffolds were obtained using a Leica SP8 confocal microscope with 10X/NA0.4, 20X/NA0.75, or 63X/NA1.4 oil immersion objectives.

doi:10.6342/NTU202403815

RNA extraction

Total RNA was extracted using a lab-optimized method with the RNeasy Plus Micro kit (Qiagen #74134), which notably did not involve gDNA separation or enzymatic DNase treatment. The optional use of 20ng carrier RNA was included during this process. RNA quality and quantity were subsequently assessed using a Nanodrop spectrophotometer (Thermo Fisher) at 260 nm and 280 nm, with an A260/A280 ratio greater than 1.80 indicating sample purity.

cDNA synthesis

In each sample, 96ng of RNA was reverse transcribed into cDNA using the SuperScript™ VILO™ Master Mix (Invitrogen #11755050) in a 20µl reaction. The reverse transcription occurred over three steps: 10 minutes at 25°C, followed by 10 minutes at 50°C, and finally 5 minutes at 85°C.

Real-time qPCR

Subsequent qPCR reactions were conducted using the CFX96 Touch Real-Time PCR Detection System (Bio-Rad) and 96-well plates (Bio-Rad #HSP9901). Each reaction was run in duplicate, with individual wells containing 9µl of cDNA template (diluted with RNase free water), 10µl of iQ™ SYBR® Green Supermix 2x (Bio-Rad #1708882), and 0.5µl primer (10µM). Details of the gene-specific primers used can be found in the primer list. The 2-step real-time PCR cycling conditions were as follows:

- Initial denaturation: 95°C for 3 minutes
- Amplification: 40 cycles of 95°C for 10 seconds and 60°C for 30 seconds
- Melting curve: 65°C to 95°C, increasing by 0.5°C every 5 seconds

doi:10.6342/NTU202403815

The relative gene expression levels were calculated using the $2^{-\Delta\Delta Ct}$ method, with normalization to the housekeeping gene GAPDH.

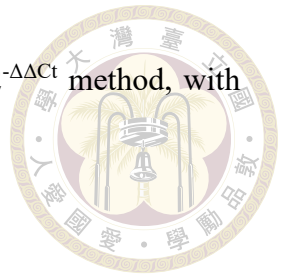

2.4. Statistical analysis

Statistical analysis was performed using Fisher's exact test or Student's t-test for datasets featuring two groups. For non-parametric data involving more than two groups, Wilcoxon tests were conducted using Benjamini-Hochberg (BH) adjustment. Results were expressed in box plots with medium, $Q_{1/4}$ and $Q_{3/4}$. For proportional test, chi-squared test (χ^2 test) was conducted with Benjamini-Hochberg (BH) adjustment.

Statistical analysis was carried out using R (R-4.4.1) or Microsoft Excel 2021. A p-value of less than 0.05 was considered statistically significant.

doi:10.6342/NTU202403815

3. Results

3.1. Primary culture system and inducible progerin expression in VSMCs

VSMCs isolated from transgenic mouse aortas and cultured according to the outlined tissue explant protocol, underwent evaluation for purity at passage 2 (P2). **Figure 4** shows immunofluorescent staining targeting VSMC contractile cell markers (α-smooth muscle actin, SM-22, and Calponin-1) revealed a high proportion of cells expressing these markers, such as more than 75% of these P2 cells expressed SM22, a VSMC-specific marker (**Figure 5**).

P1 VSMCs were treated with 4-hydroxytamoxifen (4-OHT) for 72 hours to induce progerin expression. In **Figure 4** and **Figure 5**, immunostaining for the FLAG-tag showed 98~100% of VSMCs expressed progerin after induction, while neither the negative control nor the control group displayed any progerin expression, indicating the successful induction of progerin expression in VSMCs.

doi:10.6342/NTU202403815

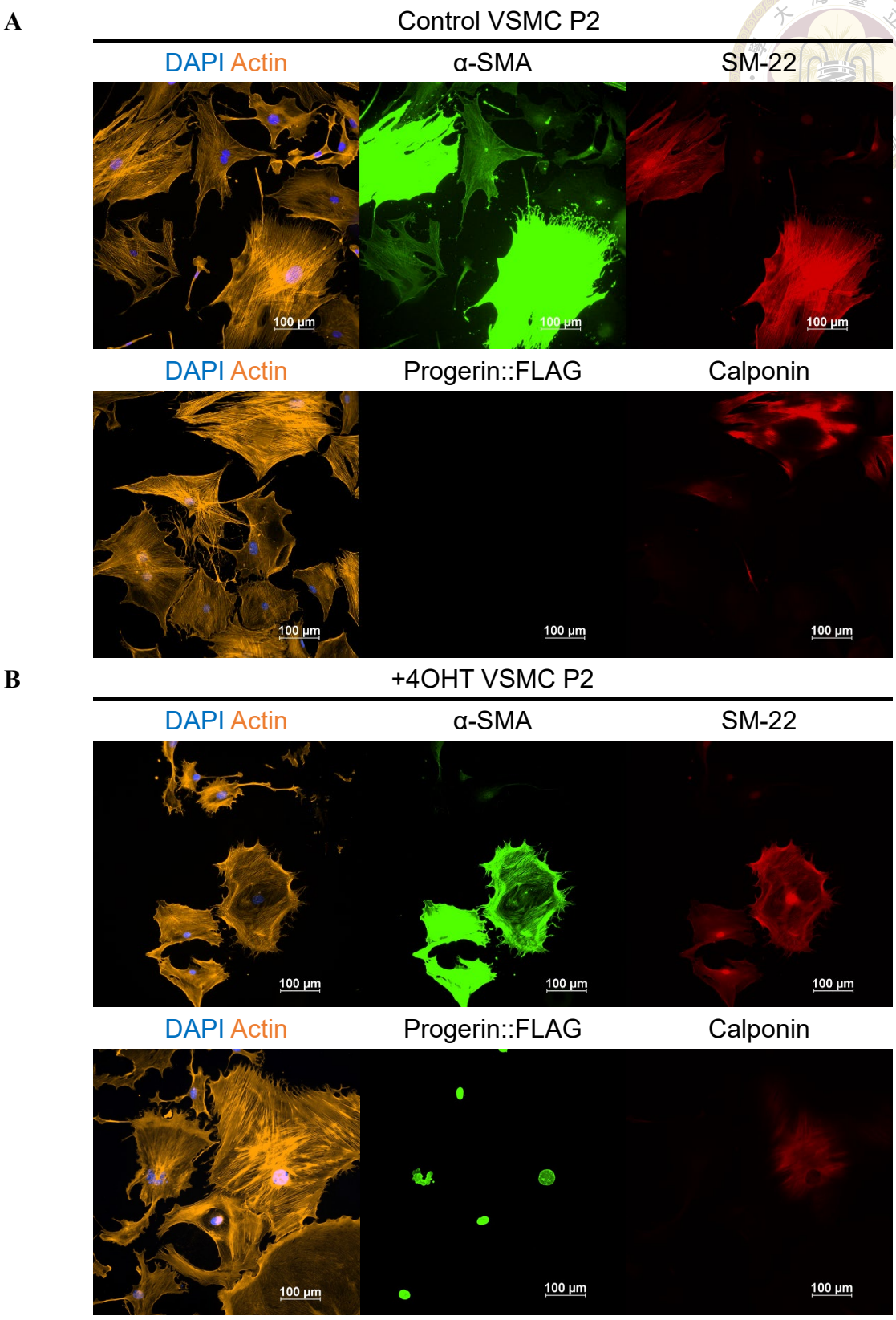

Figure 4 Immunostaining in P2 control and 4-OHT treated VSMCs in 2D culture. P2 control (A) and 4-hydroxytamoxifen treated (B) VSMCs on coverslip stain for α-SMA, Calponin and SM-22. Scale bar is 100 µm.

doi:10.6342/NTU202403815

3.2. Phenotypic change in prolonged passaging and progerin expressing VSMCs

As the passage number increased, there was a decrease in the population of cells positively stained for α-SMA, SM-22, and calponin-1, suggesting a phenotypic alteration with cell division, see **Figure 5**. In addition, contractile marker expression further decreased in the progerin-expressing cells. This suggests that progerin might contribute to the downregulation of contractile markers in VSMCs.

doi:10.6342/NTU202403815

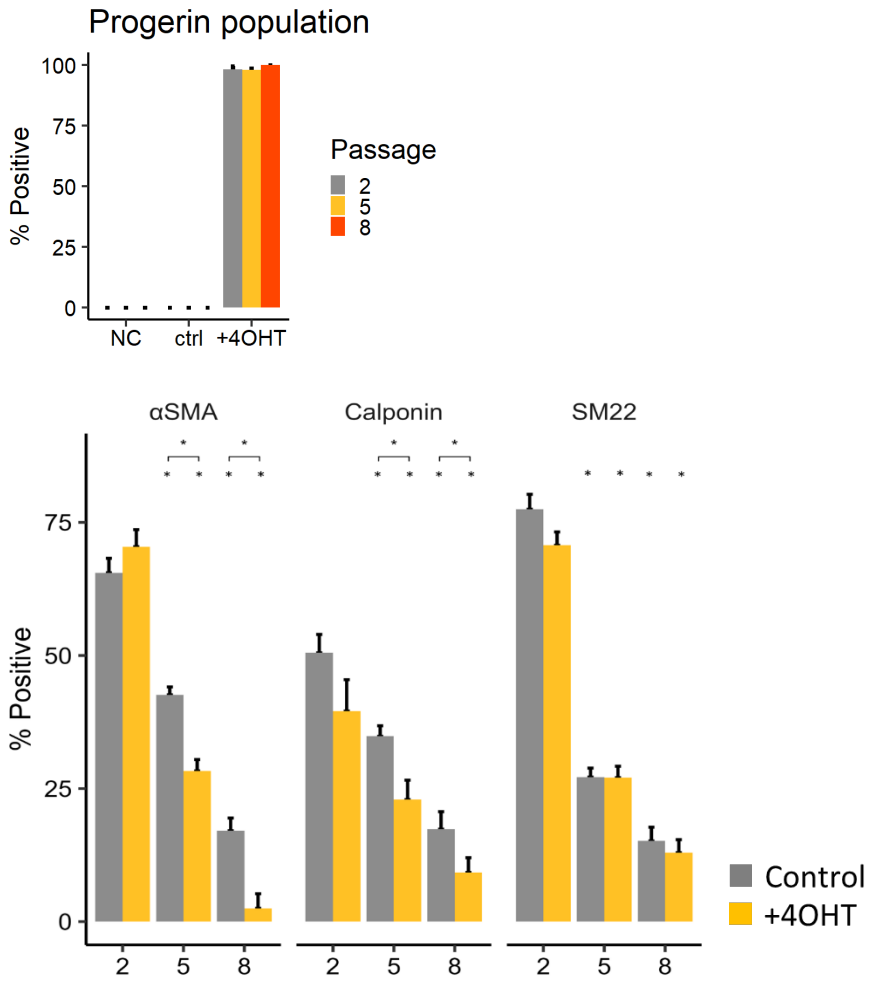

Figure 5 Immunostaining for progerin and contractile markers in passage 2, 5 and 8 VSMCs in 2D Culture.

Passage and progerin expression reduce contractile markers on VSMCs. (For sample size of P2 n>100, P5 and P8 n>150. From 7 repeats. Line indicates $p<0.05$ between each group, * indicates $p< 0.05$ compared with its group in P2).

doi:10.6342/NTU202403815

3.3. Electrospun scaffolds

Crimped fibers typically exhibit a crimpness exceeding 3%, whereas straight fibers maintain a crimpness below 3% (**Figure 6C**). The typical thickness of crimped materials ranges between 0.20798 ± 0.02252 mm, while straight materials typically measure between 0.1055 ± 0.01858 mm in thickness.

In **Figure 6**, crimped materials typically have an elasticity modulus (E) around 63.83 ± 26.29 MPa and toe region is approximately 11.68 ± 6.83%, whereas straight materials exhibit a linear mechanical behavior with a higher elastic modulus (E) measuring between 278.93 ± 67.77 MPa and toe region is approximately 0.52 ± 0.43 %. The wavy structure confers the scaffold with non-linear stress-strain behavior, featuring an extended toe region.

doi:10.6342/NTU202403815

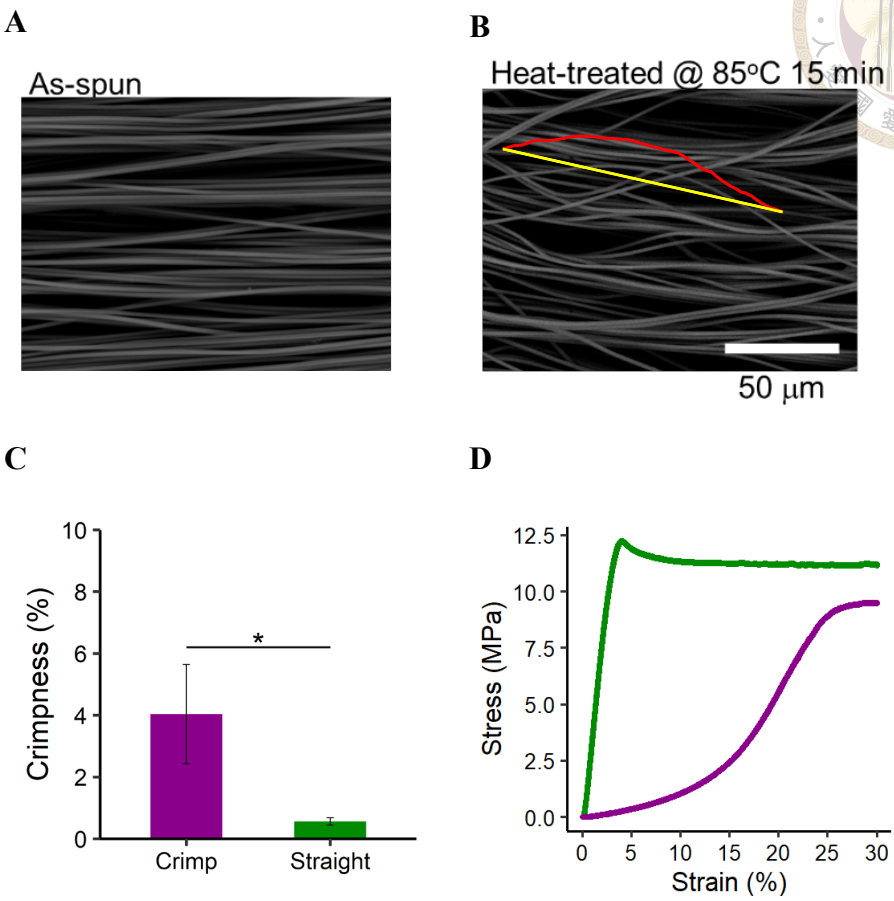

Figure 6 SEM and properties comparison of straight and crimp fibers.

(A-B) Scanning Electron Microscope (SEM) images showing straight and crimp fiber structures. Red curve indicates real length between endpoints while the yellow line represents the linear distance between endpoints (C) Measurement of crimpness, each fiber measure with 20 repeats. (D) Representative tensile stress-strain curve comparing straight and crimp fiber. Scale bar= 50 μm.

doi:10.6342/NTU202403815

3.4. Modulation of VSMCs phenotype by fiber structure, passage and progerin expression

We cultured P3, P6 and P9 VSMCs with or without progerin expression on straight and crimp fiber to probe the interaction of intrinsic and extrinsic factors on aging. VSMCs on fibrous culture displayed elongated morphologies, while cells on crimp fiber showed a more spread-out morphology. Cell nucleus also had elongated morphologies.

Similar with previous VSMC 2D culture, the proportion of VSMCs expressing contractile markers (α-SMA and calponin) decreased with increasing passage numbers. Additionally, progerin expression further reduced the proportion of VSMCs with contractile markers, indicating its potential role in modulating VSMC phenotype.

Figure 7 revealed that VSMCs on straight fibers exhibit a notable decline in α-SMA and calponin expression compared to those on crimped fibers, across all passages examined. The decline became more pronounced with increasing passage number and progerin expression, indicating that these factors significantly accelerate the phenotypic deterioration of VSMCs on straight fibers. This underscores the combined impact of scaffold architecture, passage number, and progerin expression on VSMC phenotypic decline.

doi:10.6342/NTU202403815

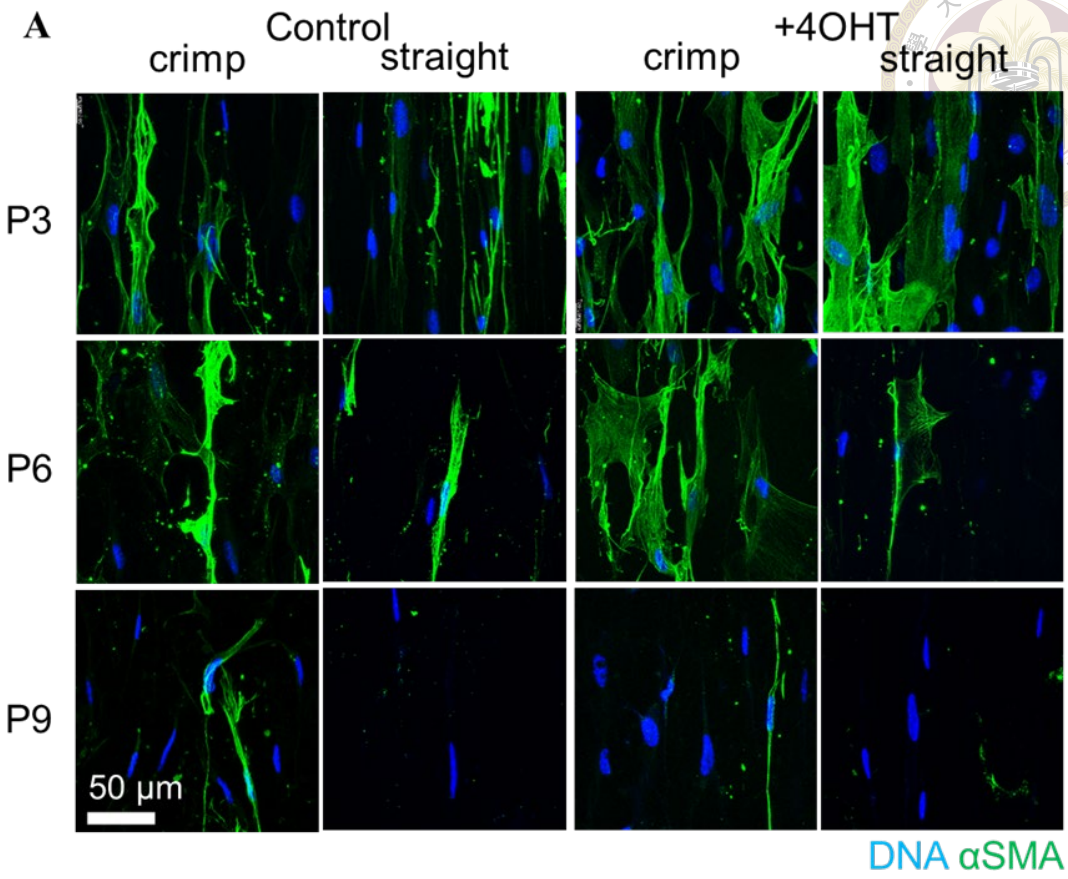

doi:10.6342/NTU202403815

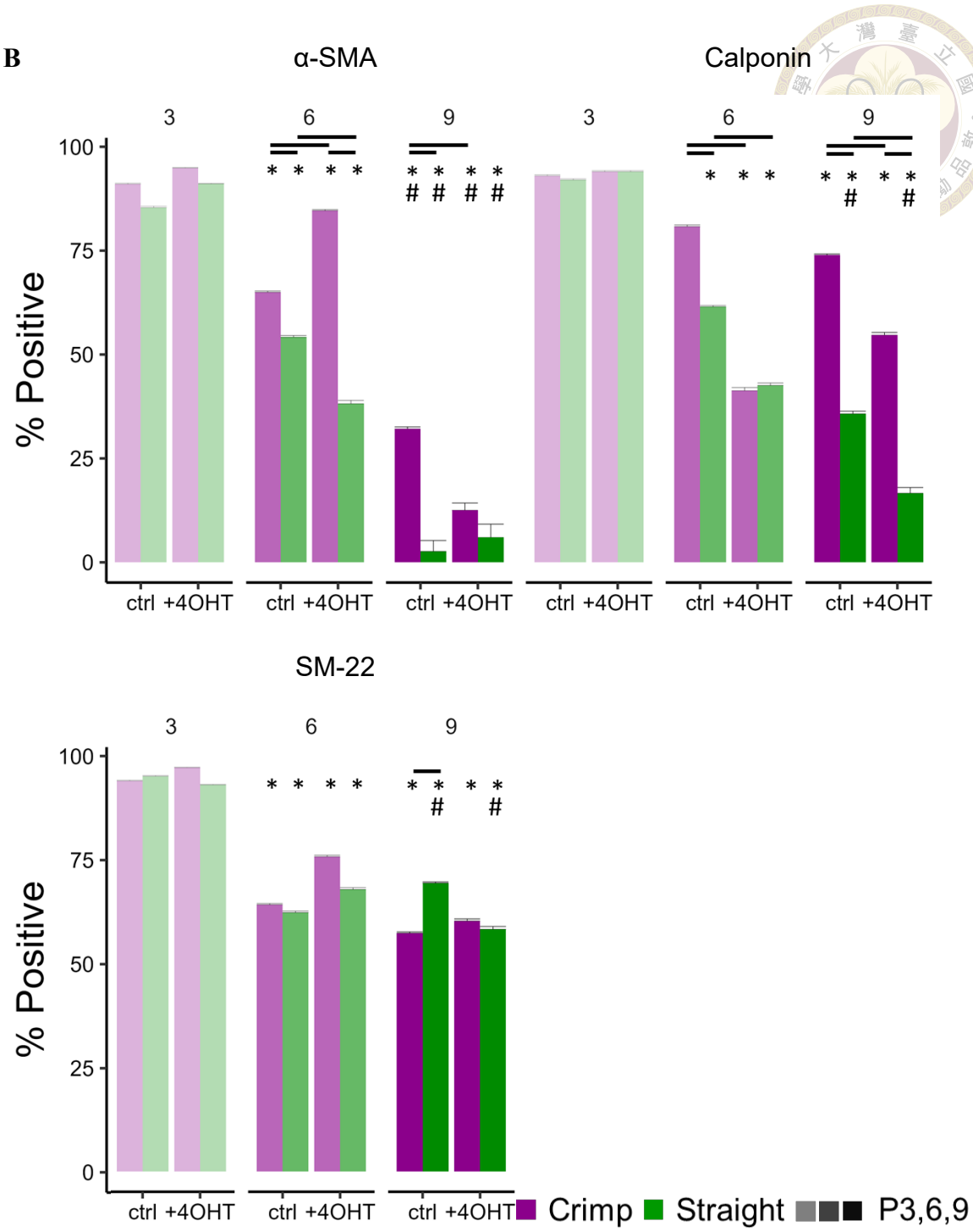

Figure 7 Immunostaining for αSMA in passage 3, 6 and 9 VSMCs on 3D straight and crimp fiber.

(A) Confocal images from passage 3, 6 and 9 VSMCs with or without 4OHT induced progerin expression. (B) Quantification of marker-positive VSMCs. P3, 6, 9 n>150. Scale bar is 50 μm. Line indicates $p<0.05$ between each group, * indicate $p< 0.05$ compared with P3, # indicate $p< 0.05$ compared with P6.

doi:10.6342/NTU202403815

One behavior of synthetic VSMCs is enhanced proliferation. In this study, we investigated the effects of fiber structure and progerin expression on the proliferation of VSMCs. Utilizing Alamar Blue assay, we assessed cell proliferation in VSMCs from passages 3, 6, and 9, with and without progerin expression, cultured on wavy and straight fibers. **Figure 8** revealed that both cell passage and progerin expression increased VSMC proliferation. Interestingly, in P6 progerin-expressing cells, proliferation was suppressed by wavy scaffold, while in P6 control cells, fiber structure did not alter proliferation. Furthermore, P9 VSMCs exhibited an increased proliferation rate across all groups compared to P3 and P6, and the influence of fiber structure still persisted. However, effect of progerin was not significant. Crimp fiber demonstrated a suppressive effect on cell proliferation in dedifferentiated VSMCs by progerin expression or serial passages.

These results underscore the intricate interplay between fiber structure, progerin expression, and VSMC proliferation. We observed that in young and healthy VSMCs (P3), neither progerin expression nor fiber structure significantly influenced proliferation or contractile marker expression. However, in the transitional state of middle age (P6), crimp fiber demonstrated a rescuing effect specifically on progerin-expressing VSMCs, indicating passage-dependent susceptibility to progerin-induced changes. Conversely, in late passage (P9), progerin introduction did not exacerbate VSMC pathology, and crimp fiber exhibited a recovery effect on both progerin-expressing and control VSMCs. These findings highlight the passage-dependent interplay between fiber structure, progerin expression, and VSMC phenotype.

doi:10.6342/NTU202403815

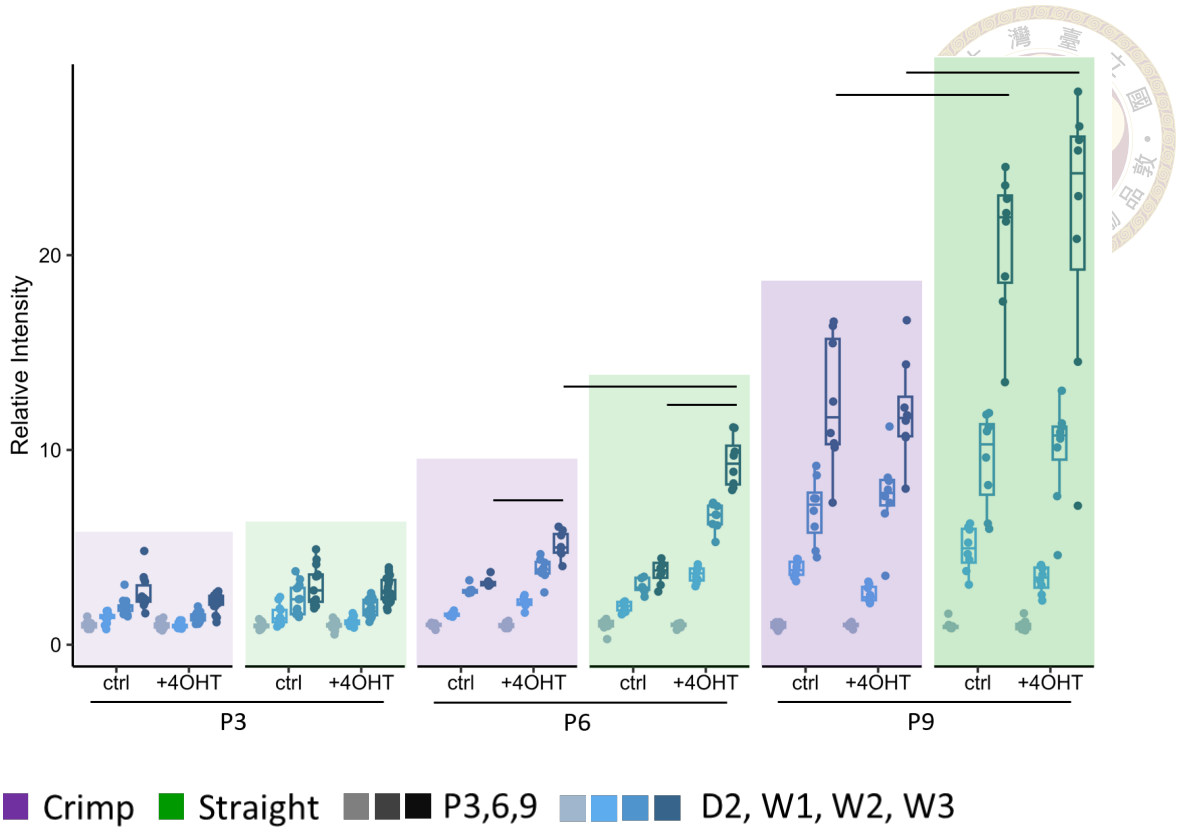

Figure 8 P3, 6 and 9 VSMCs proliferative profile in 3D culture.

Within each cell of passages, W1~3 data were normalized to its D2 and D2 data were normalized to means of D2. Line indicates $p < 0.05$ between W3 of each group.

doi:10.6342/NTU202403815

3.5. Dynamic loading system

In previous study [57], we built a custom uniaxial tensile bioreactor. The displacement was calibrated using a thin polydimethylsiloxane (PDMS) film and was analyzed using ImageJ. The strain in the PDMS film was confirmed using markers in successive images. When stretched, X-axis strain is approximately 8.78%, and Y-axis strain is approximately -3.19% when the system was subjected to a 10% strain (**Figure 9**). Subsequently, a dynamic loading of 10% strain at 1 Hz frequency was applied for 3 hours to assess system stability, resulting in final X-axis strain approximately 6.23% and Y-axis strain is approximately -2.85%.

doi:10.6342/NTU202403815

A

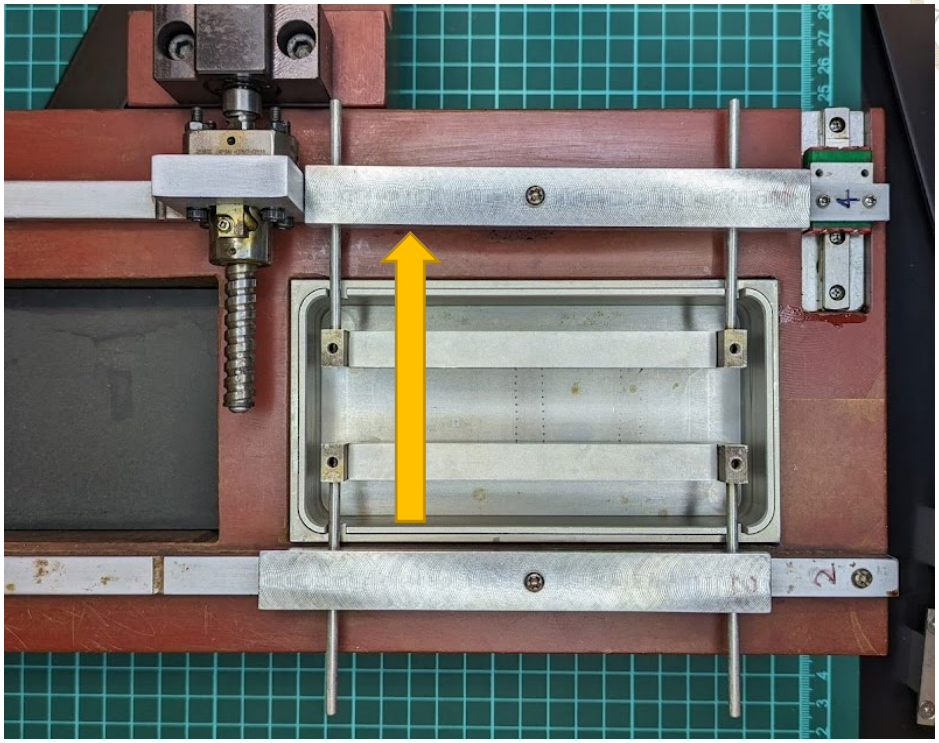

B

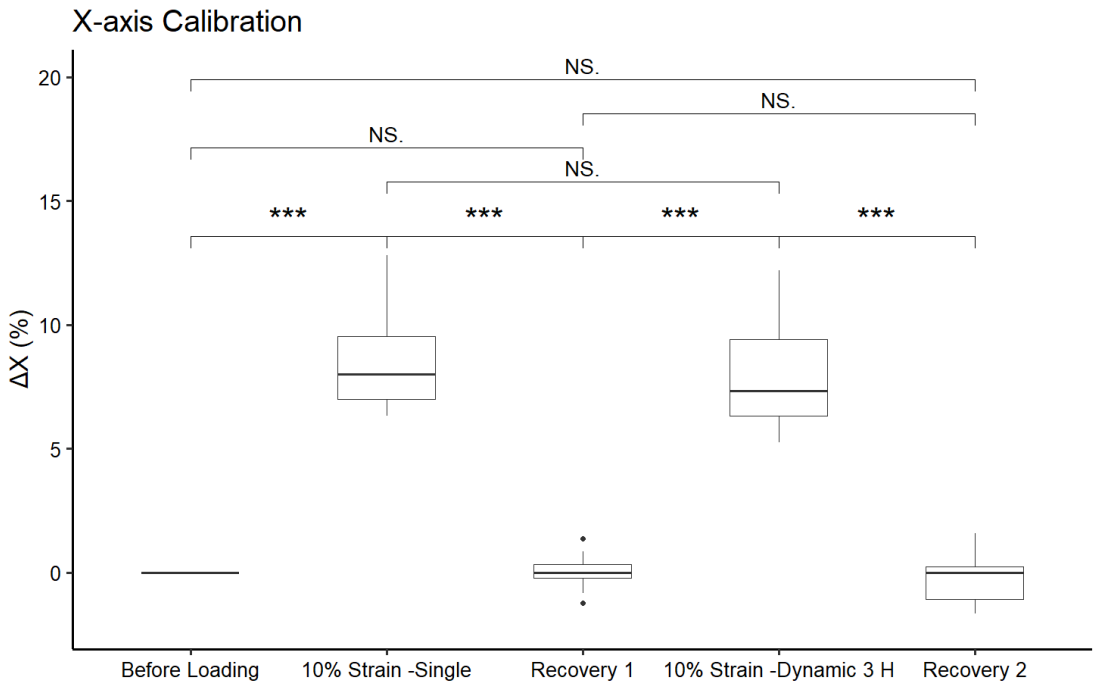

doi:10.6342/NTU202403815

C

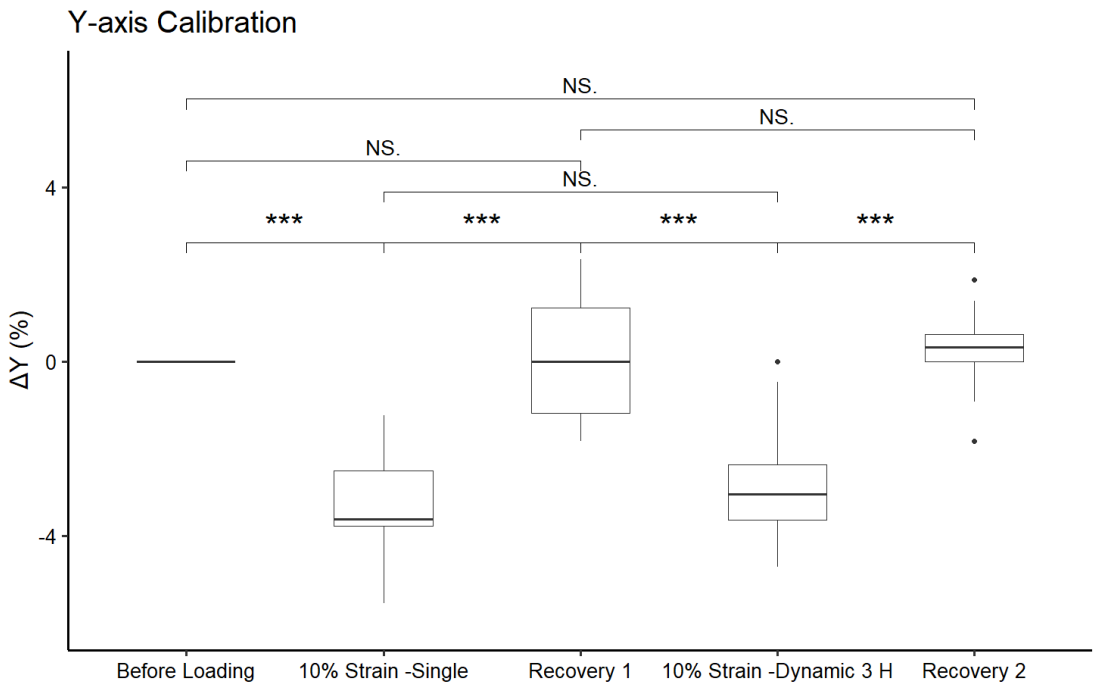

Figure 9 Bioreactor calibration results after the application of 10% strain, either as a single instance or dynamically for 3 hours at 1 Hz.

(A) Custom bioreactor with PDMS membrane for calibration. Yellow arrow indicates the strain direction. (B-C) Comparison of bioreactor calibration results of X and Y axis under two conditions: 10% strain applied once (10% Strain -Single) and 10% strain applied dynamically for 3 hours at 1 Hz (0% Strain -Dynamic 3 H). 18~20 points for calibration in each movement.

doi:10.6342/NTU202403815

3.6. Effects of dynamic loading

P6 and P9 VSMCs, with and without progerin, were cultured on crimp and straight fiber scaffolds for three weeks. Subsequently, individual samples were transferred to a bioreactor for dynamic loading experiments. We applied 0%, 4% or 10% strain for 3 hours on crimp fibers. Due to the mechanical properties of straight fibers, only 0% and 4% strain were applied to them. In VSMCs, contractile genes such as *Acta2, Taglin, Cnn1,* and *Myh11* indicate a contractile, differentiated state focused on contraction. In contrast, synthetic genes like *Spp1, Klf5,* and *Col1a1* are associated with a synthetic, proliferative, or transitional state that is involved in tissue repair, ECM production, and remodeling.

In our analysis of contractile gene expression, we found that the expression levels of *Acta2* and *Taglin* generally increased with mechanical strain (4% and 10%). Notably, *Acta2* expression decreased in progerin-expressing groups compared to controls. **Figure 10** shows that in the P6 static (0% strain) group, the straight fibers led to lower *Acta2* and *Cnn1* gene expression in VSMCs, which is consistent with our immunostaining results (**Figure 5** and **Figure 7**). However, in P9 static group there are no significant *Cnn1* expression difference between two types of fibers. There was no significant difference contributed by fiber type nor progerin in *Taglin* expression. Interestingly, when progerin expression was combined with dynamic stain, the *Taglin* expression was further enhanced. Regarding passages, *Acta2 and Cnn1*expression levels in crimped fiber tended to be lower in P9 compared to P6. *Myh11* exhibited less consistent patterns, showing some decrease with strain in certain conditions but often increased in progerin-expressing groups.

Examining the synthetic markers, *Spp1* (Osteopontin) showed a significant increase in +4OHT groups, especially at P6. *Spp1* expression levels were generally higher in control cells in P9 compared to P6. *Klf5*, a key transitional transcriptional factor, increased with mechanical strain. It showed generally lower expression in progerin-expressing

doi:10.6342/NTU202403815

groups, particularly at P6. The extracellular matrix protein *Col1a1* decreased in control VSMCs when subjected to dynamic strain, but progerin-expressing can diminish the *Col1a1* downregulation by dynamic strain. *Col1a1* decreased in control VSMCs when cultured on straight fiber, while the effects of passage on *Col1a1* expression were less pronounced.

General observations across all genes revealed the effect of progerin expression being more pronounced at P6 for most genes. Prolonged passage decreased *Cnn1* gene expression and upregulated *Spp1* and *Klf5* genes. Mechanical loading significantly impacted the expression of contractile genes, particularly upregulating *Acta2* and *Taglin*, as well as synthetic genes such as *Klf5*. Progerin expressing decreased certain expression of contractile gene *Acta2* and *Klf5* in P6, while increasing expression of synthetic genes *Spp1* in P6. Differences between crimped and straight fibers were observed but were not consistent across all conditions and genes.

These results demonstrate complex gene expression patterns in VSMCs in response to mechanical strain, progerin expression (+4OHT), passage number, and fiber geometry. The data suggest a shift towards a less contractile phenotype with progerin expression, straight fiber and latter passages. However, the crimp scaffolds and mechanical strain can contribute VSMC more contractile phenotype.

doi:10.6342/NTU202403815

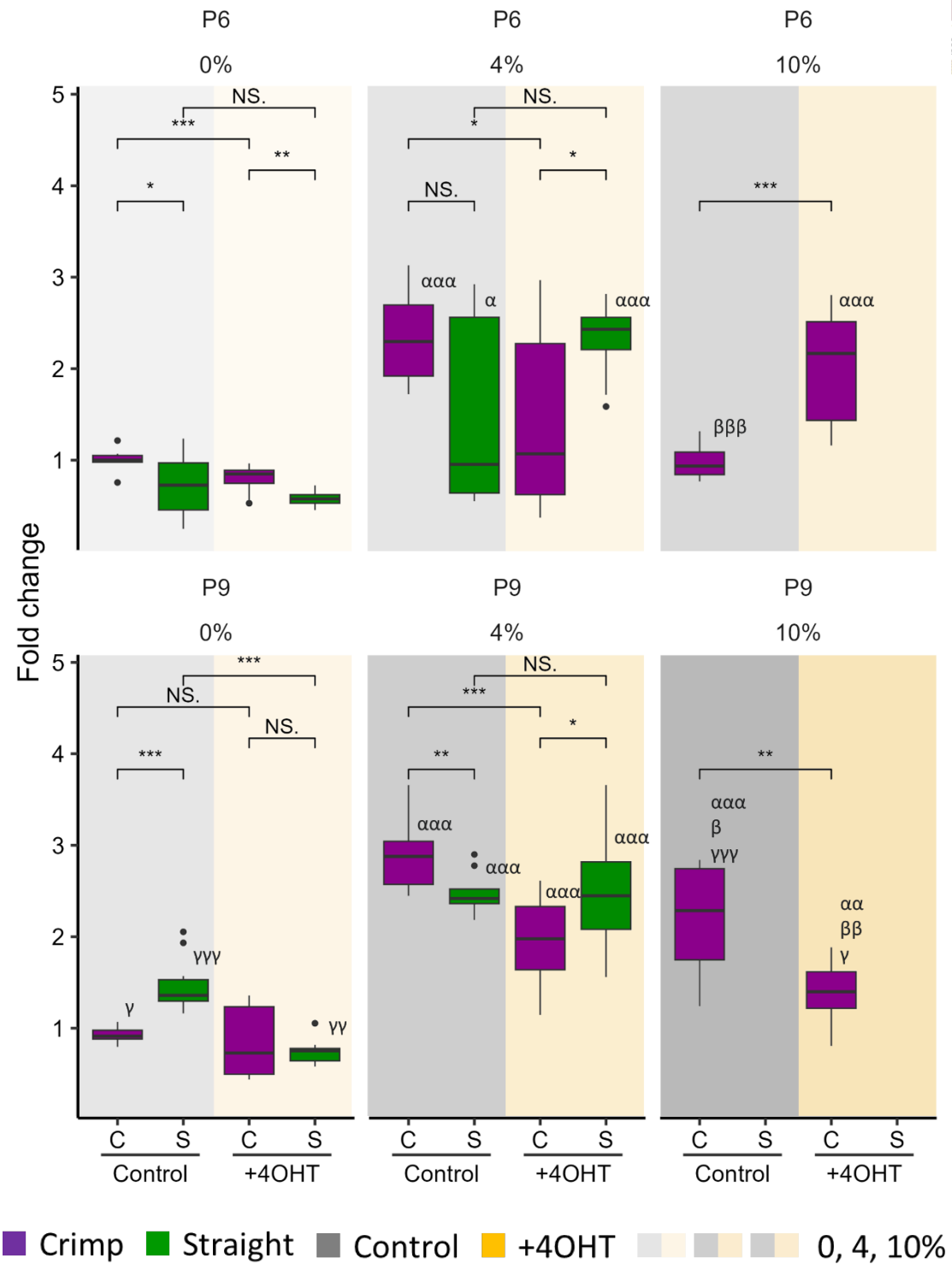

doi:10.6342/NTU202403815

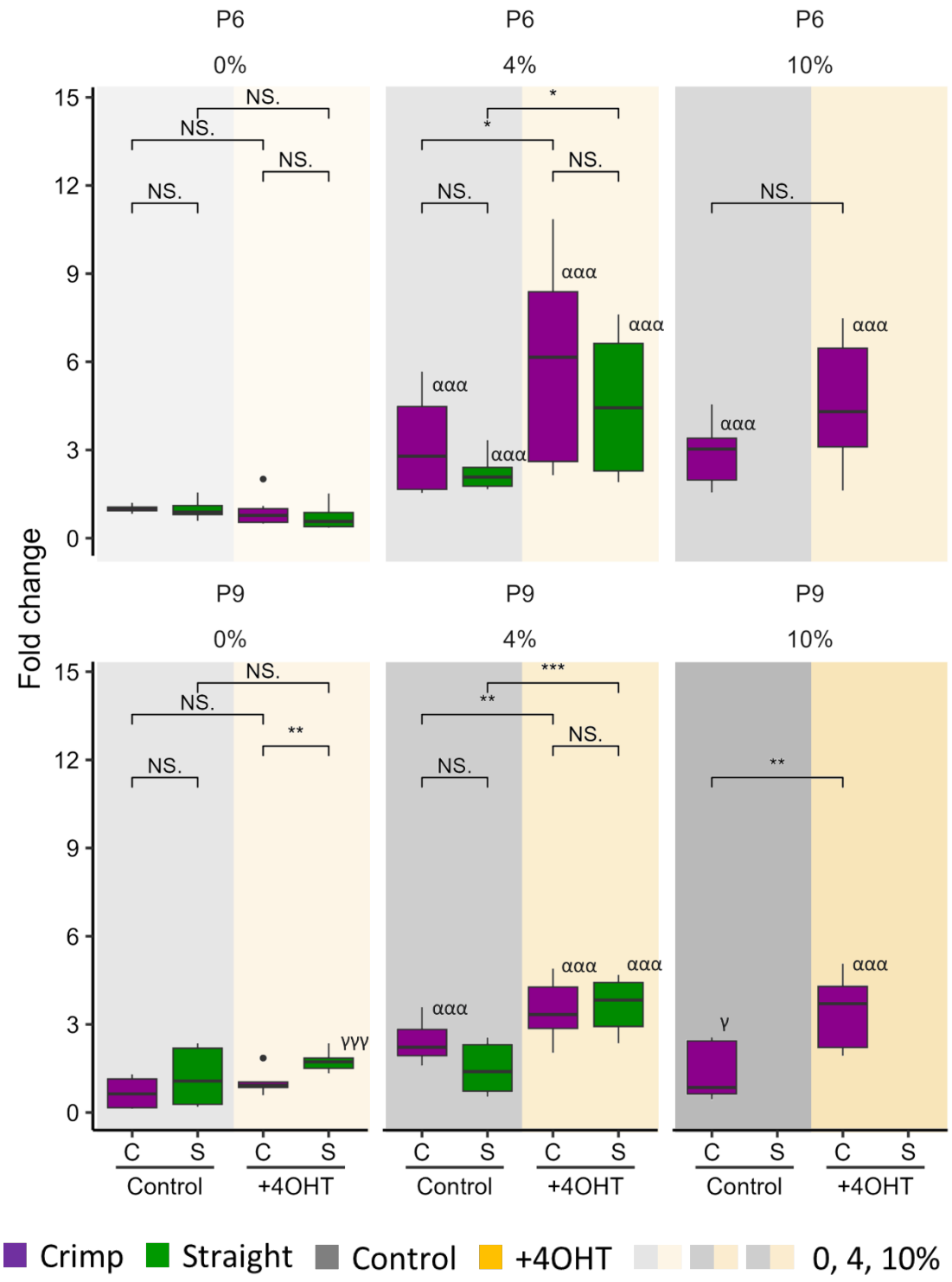

doi:10.6342/NTU202403815

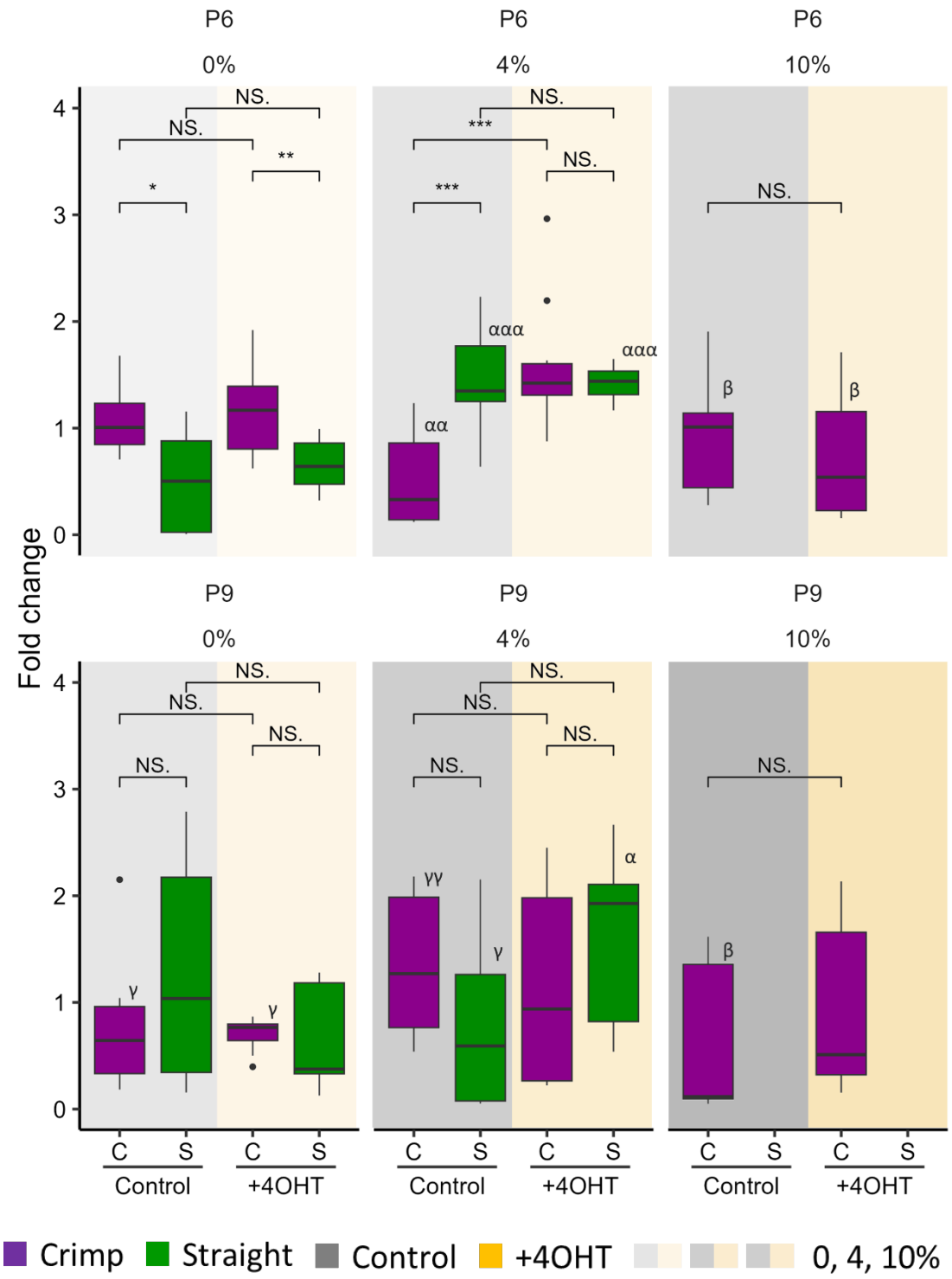

doi:10.6342/NTU202403815

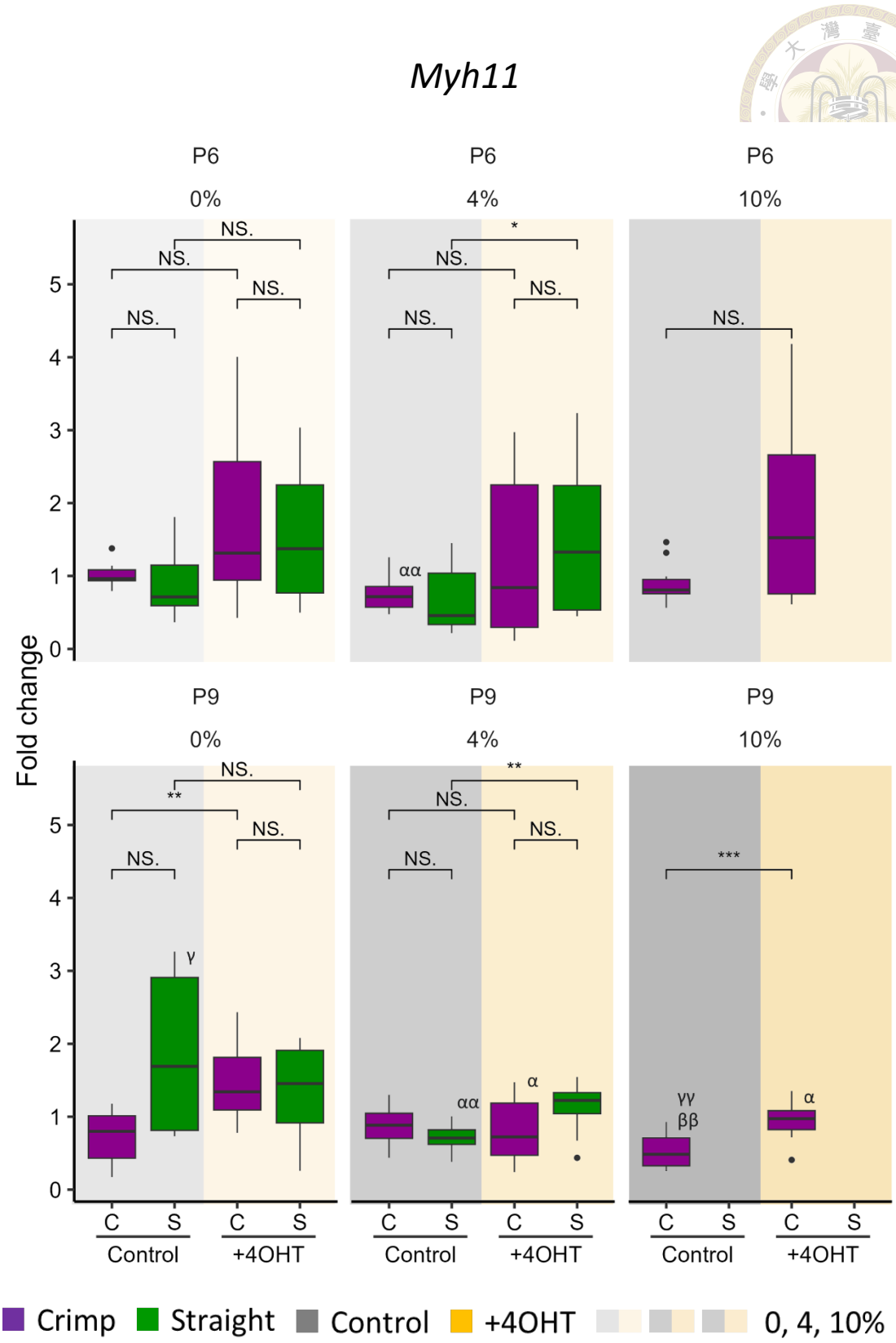

doi:10.6342/NTU202403815

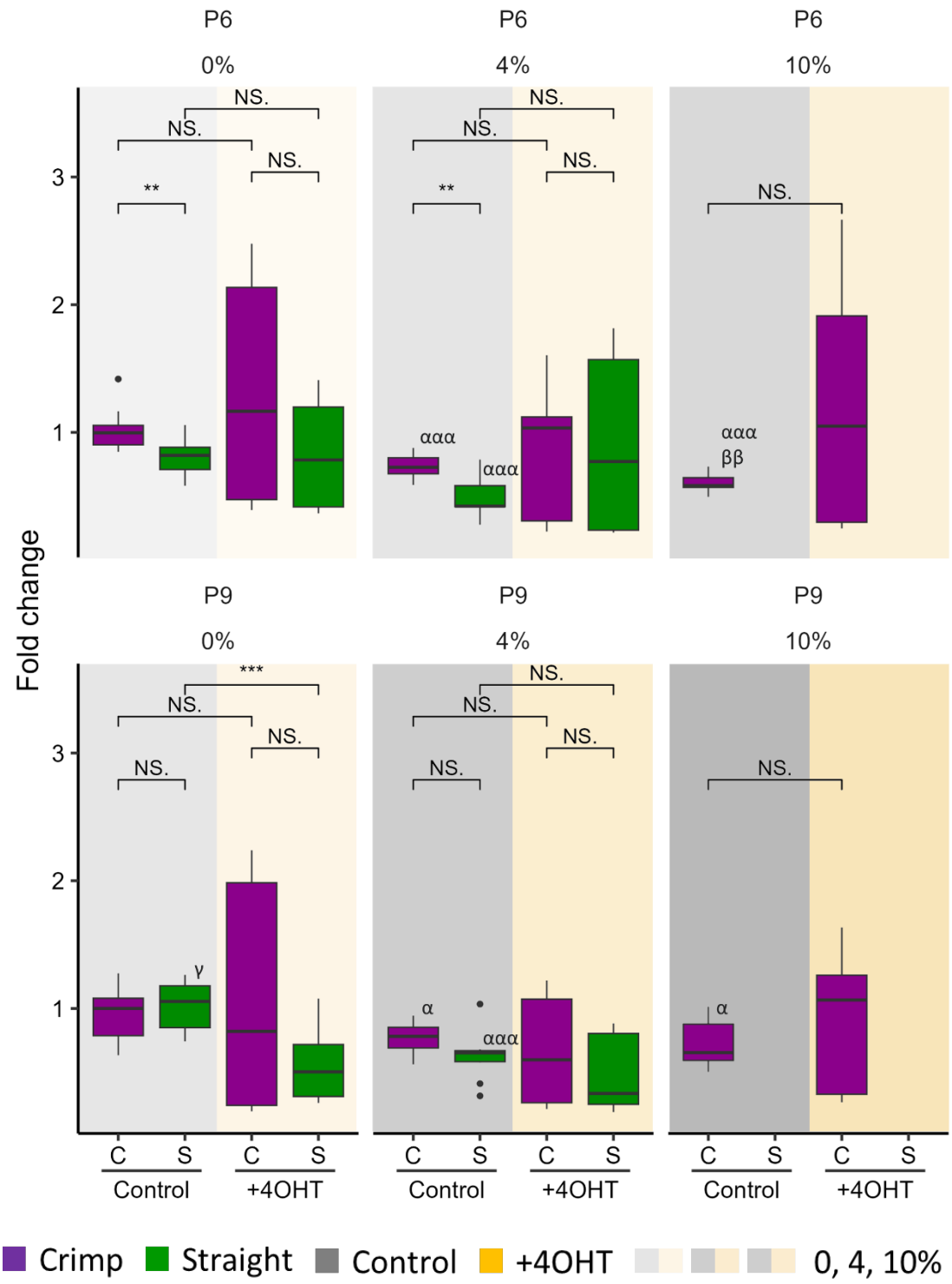

doi:10.6342/NTU202403815

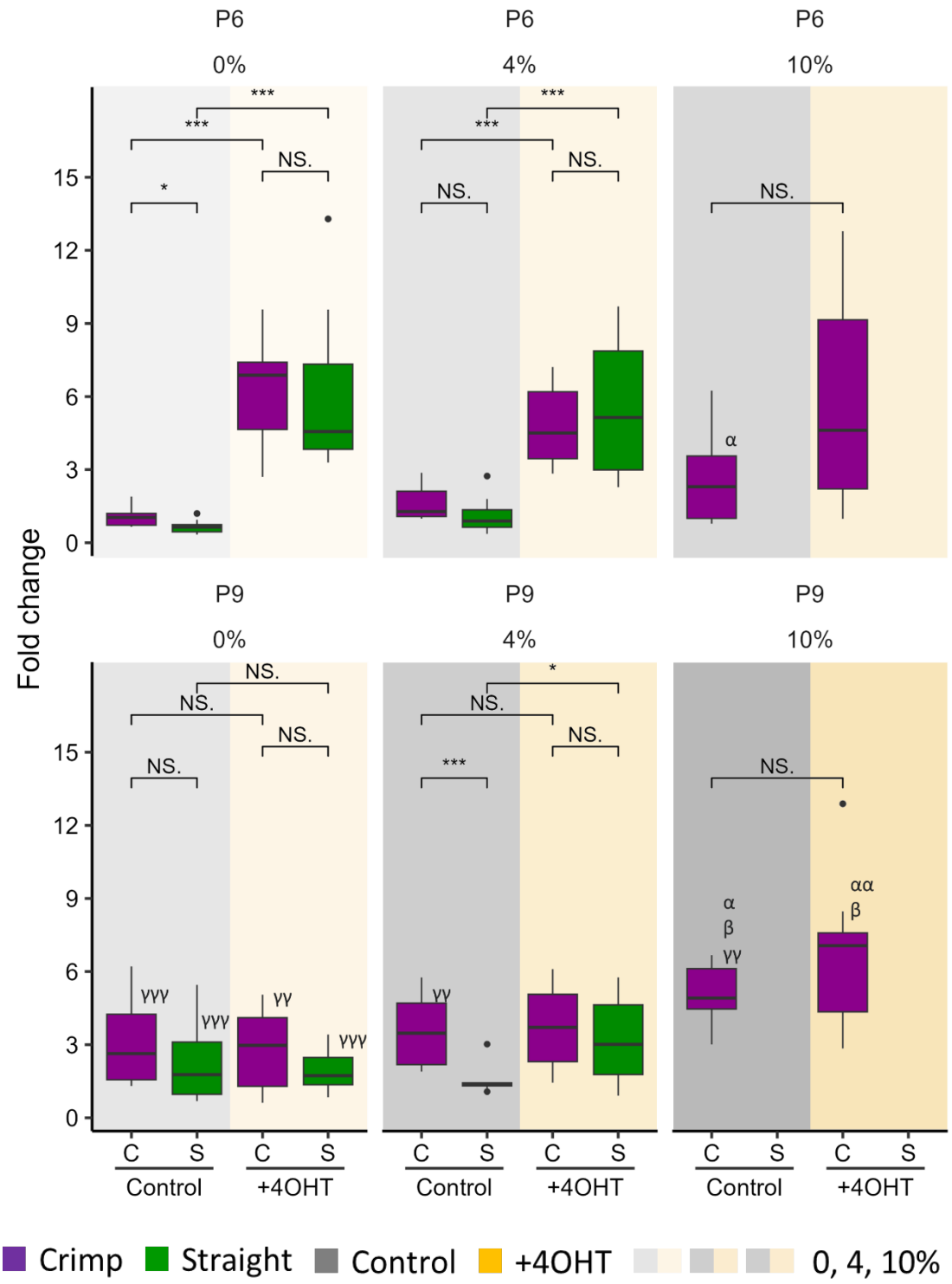

doi:10.6342/NTU202403815

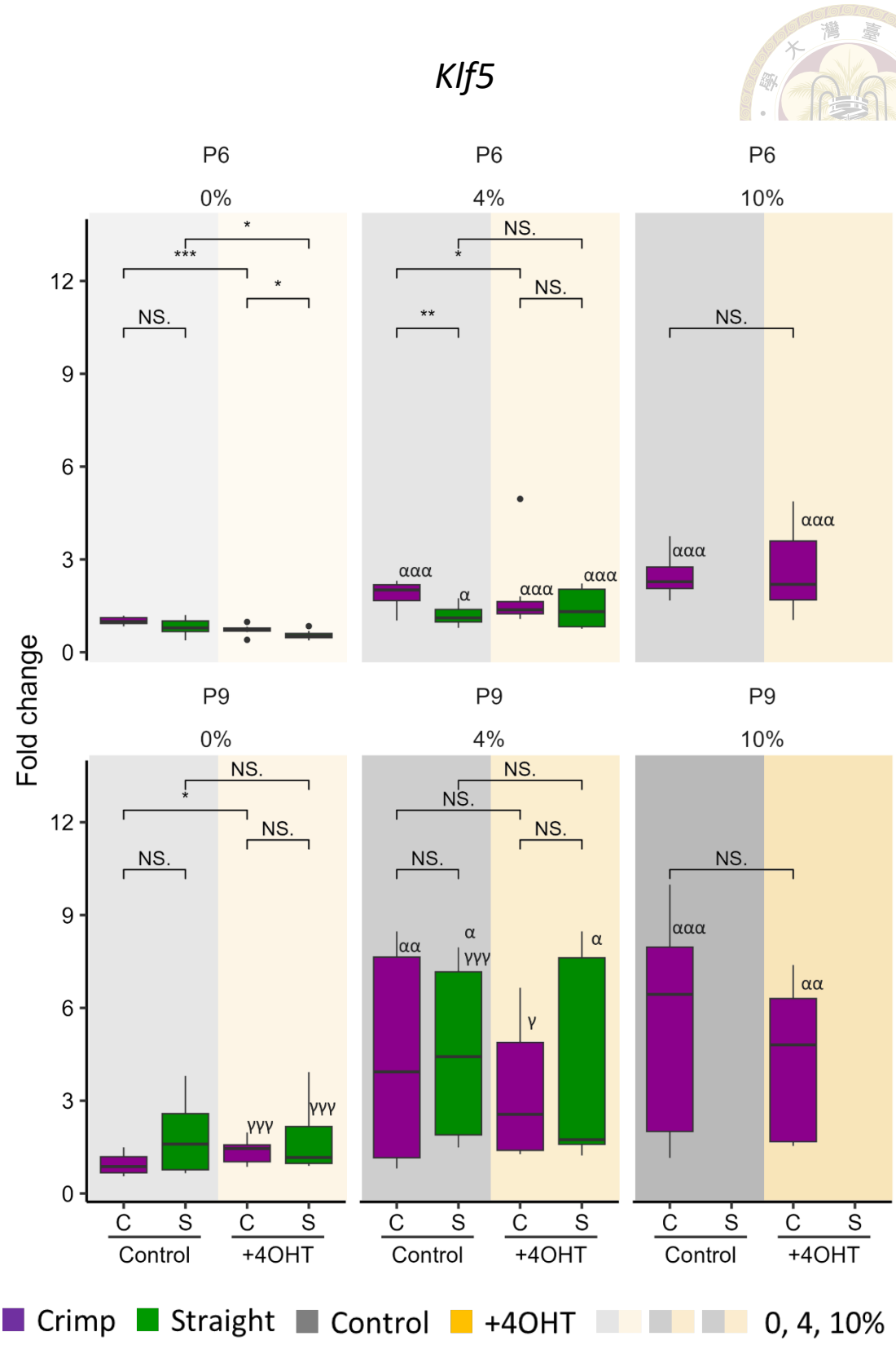

Figure 10 Contractile and synthetic gene expression across crimp and straight fibers, cell types, dynamic loading strains, and passages.

The figure shows the fold change in gene expression for different treatments (fiber: crimp

doi:10.6342/NTU202403815

and straight; cell: negative control and 4OHT treated VSMCs; dynamic loading strains: horizontal 0%, 4%, 10% at 1 Hz). The top and bottom panels represent the results from passages P6 and P9, respectively. Statistical significance is indicated by horizontal bars: * $p < 0.05$, ** $p < 0.01$, *** $p < 0.001$, and NS indicates no significance. For significance between groups, α indicates a comparison with the static group, β indicates a comparison with the 4% strain group, and γ indicates a comparison with the P6 group. Each group n=5~7, batch repeats =2.

doi:10.6342/NTU202403815

4. Discussion

Aging is a gradual process of deterioration in cells, tissues, and overall physiological functions over time. In vivo research has shown that aging induces morphological changes in the aorta, which affect populations suffering from hypertension and atherosclerosis [12]. This process also leads to increased aortic stiffness, reduced arterial compliance, and decurved elastic fibers [47, 58-60]. Instead, type I collagen becomes more prevalent and this shift in the collagen-elastin balance contributes to arterial stiffening [50, 58]. In addition, the aging process causes elastin lamina structure to flatten and become fragmented [58, 61]. We also observed this phenomenon in cross-sectional arterial sections from both young (10-week-old) and old (84-week-old) mice in **Figure 2**. Therefore, we hypothesize that changes in fiber microstructure are responsible for the phenotypic modulation of VSMCs. To test this hypothesis, we designed wavy and straight fiber structures to simulate healthy/young and pathological/aged arterial architectures. In our results, the combination of progerin expression, straight fiber structures, and later passage numbers results in significantly worse outcomes, suggesting interactions among these factors that further impair VSMC health.

VSMCs undergo phenotypic modulation during aging, transitioning from a contractile to a synthetic phenotype [13, 58, 62, 63]. In our study, we found that several VSMC key contractile proteins or genes such as αSMA (*Acta2*), SM-22 (*Taglin*) and Calponin-1 (*Cnn1*) decreased with increased culture passage and progerin expression (**Figure 5**, **Figure 7** and **Figure 10**). Our results are consistent with findings from multiple studies [62, 64-67].

doi:10.6342/NTU202403815

When cultured on straight fibers to simulate the aging/pathological structure compared with VSMCs cultured on crimp scaffolds, the population expressing contractile markers αSMA and calponin decreased (**Figure 7**). These results suggest the straight microenvironment causing VSMCs to become less contractile. Moreover, the synthetic VSMCs tend to be more proliferative on straight fibers (**Figure 8**). The synthetic phenotype is considered a de-differentiated state of VSMCs, exhibiting enhanced proliferation and migration capabilities compared to their contractile counterparts [12]. This phenotypic change is a significant indicator, often observed in the context of vascular injury and disease [12, 63]. The observed decrease in contractile protein expression implies that these VSMCs were less effective at regulating blood vessel diameter, impacting blood pressure and flow, potentially contributing to vascular dysfunction [31, 68]. An increase in VSMC proliferation usually signifies that the cells responded to repair damaged blood vessels [62]. However, excessive or prolonged proliferation can be detrimental, leading to the thickening of blood vessel walls and potential blockages [62].

In addition to passage number, progerin provides an alternative means of inducing cellular aging. Progerin, a mutated form of the Lamin A protein, is a valuable tool for studying cellular aging due to its role in Hutchinson-Gilford progeria syndrome (HGPS), a condition that mirrors accelerated aging [10, 11]. The vicious impacts from progerin aggravate VSMC to lose contractile genes and proteins and enhance cell proliferation (**Figure 5**, **Figure 7**, **Figure 8** and **Figure 10**). These results correspond with the established understanding [13, 29, 38, 68, 69].

VSMCs are constantly exposed to mechanical stress in vivo, which significantly impacts their function, phenotype, proliferation, migration and alignment [12, 29, 43, 62, 63]. To further understand how these mechanical stresses affect VSMC behavior, we designed experiments to simulate this physical environment and study the effects of

doi:10.6342/NTU202403815

progerin expression, fiber structure, and passage. In our VSMCs gene profiles on static fibrous scaffold (**Figure 10**), progerin expression caused *Acta2* gene down-regulation and *Spp1* gene up-regulation. Osteopontin, encoded by *Spp1* and also known as Secreted phosphoprotein 1, is a protein involved in the adhesion of osteoclasts to the mineralized bone matrix [70]. *Spp1* is involved in the calcification process of atherosclerotic plaques, which can lead to heart failure [70, 71]. Recent research has highlighted the potential role of *Spp1* in mediating interactions between immune cells and vascular calcification [70].

The simultaneous observation of progerin expression, *Spp1* up-regulation, and *Col1a1* slight up-regulation suggested that our system can recapitulate key molecular events associated with vascular calcification. Future studies incorporating functional tests for calcification, such as calcium deposition assays, would provide direct evidence to confirm this capability. Additionally, since vascular calcification is often associated with inflammation [50, 72], incorporating pro-inflammatory assays would further strengthen the system's ability to model this complex process.

Applying dynamic strain on VSMCs increased the expression of contractile genes such as *Acta2 and Taglin* (**Figure 10**), corroborating earlier research [73-75]. Applying dynamic strain also enhanced *Klf5* expression (**Figure 10**), a key transitional transcriptional factor for VSMCs phenotypic change, cell proliferation, ECM remodeling, angiogenesis, tumorigenesis and embryonic development [76-78]. We found that *Cnn1* was downregulated in our P6 control with 4% strain on crimp fiber. Conversely, we also observed *Cnn1* was upregulated in our P6 straight fiber with 4% strain and P9 progerin VSMC on straight with 4% strain. However, 10% strain didn’t contribute significant difference on both P6/9 control or progerin VSMCs. This may result from several factors, including interactions between our treatment factors and further studies should clarify this disparity. Mixed results have been reported in the literatures regarding the effects of

doi:10.6342/NTU202403815

stretch on *Cnn1* [73, 74, 79], which can be attributed to variations in experimental parameters such as strain intensity, frequency of stretch, duration of stretch, artery source, mouse strain, and ECM protein coating [43].

Progerin expression and mechanical loading primarily influence the expression of contractile genes, depended on cell passage and fiber structure (**Figure 10**). Recent researches provide evidence suggesting how progerin negatively affects VSMC mechanosensing and mechanotransduction from various ways, ultimately contributing to vascular dysfunction. VSMCs are constantly subjected to mechanical stress from blood flow. While healthy cells respond to this by increasing Lamin A/C expression and altering its nuclear localization, progerin-expressing cells show abnormal responses, leading to cell damage and death [68, 80, 81]. This heightened vulnerability might be due to progerin-induced changes in the expression of proteins crucial for cytoskeleton organization, mechanotransduction, and ECM production [82, 83]. Progerin expression disrupts the normal function of the cytoskeleton, a critical player in mechanotransduction, which likely impairs the transmission of mechanical signals from the ECM to the nucleus by disrupting the cytoskeleton and its connection to the nucleus [80, 81]. Additionally, the linker of nucleoskeleton and cytoskeleton (LINC) complex, which acts as a bridge between the cytoskeleton and the nuclear lamina to facilitate the transmission of mechanical forces to the nucleus, is negatively affected by progerin expression. This disruption in the LINC complex impairs the expression and mobility of its nuclear membrane proteins, thereby compromising the nucleus's ability to sense and respond to mechanical cues from the surrounding environment [48, 84, 85]. Furthermore, progerin expression directly increases nuclear stiffness, making the nucleus less responsive to mechanical forces and hindering its ability to deform and regulate gene expression appropriately [71, 82, 86].

doi:10.6342/NTU202403815

These multifactorial interactions highlight the complex relationships among these variables and underscore the importance of considering multiple factors together. The four-way interaction among progerin expression, fiber type, mechanical loading, and passage number is significant. This highlights the differential responses of cells at various cell aging or pathological stages to mechanical strain, which is crucial for understanding the aging process and designing treatment strategies. Future research should investigate the molecular mechanisms behind these interactions to elucidate gene regulatory networks under different conditions, aiding in the design of more effective tissue engineering and therapeutic strategies, and providing deeper insights into cellular behavior and gene regulation.

In our preliminary tests, we attempted to induce senescence in mouse VSMCs using hydrogen peroxide, referencing existing protocols [87-89]. However, we were unable to successfully detect senescence via SA-βgal staining on our mouse VSMCs. This may be attributed to the enhanced DNA repair mechanisms, higher telomere stability, and stronger mitochondrial antioxidant defenses in mouse VSMCs compared to other models [90-92]. Our lab is continuing to explore alternative pharmacological inducers of VSMC senescence, such as doxorubicin [93, 94], in an effort to overcome these challenges.

VSMCs are known for their remarkable ability to dedifferentiate from a contractile phenotype to other phenotypes, including fibroblast-like VSMCs [12, 13, 95]. However, the three-layered structure of arteries makes it difficult to achieve complete cell separation during primary culture, raising concerns about contamination from other cell types [58]. A key question is whether the observed shift in cell phenotype in our cultures could be partly due to an increased proportion of rapidly proliferating fibroblasts or endothelial cells. To address this, we have adopted methods from the literature to enhance VSMC purity. These include: First, physical removal of the adventitia (a primary source of

doi:10.6342/NTU202403815

fibroblasts) and intima (containing fibroblasts and endothelial cells) during artery dissection. Second, use of VSMC-optimized growth media and FBS concentrations. Third, verification of VSMC purity in early passages using immunostaining for markers such as α-SMA, SM-22, and calponin.

Our findings demonstrate a reduction in the contractile phenotype, consistent with observations in other studies [13, 52, 62, 96]. Additionally, we are currently experimenting with different attachment methods [97] to preferentially retain VSMCs while limiting fibroblast adherence, and may consider employing cell sorting techniques to further separate VSMCs from fibroblasts if necessary. Furthermore, we are collaborating with Professor Yang from the Department of Pharmacology at National Taiwan University to explore the use of lineage tracing techniques. This collaboration aims to track and isolate VSMCs, observe phenotypic changes over passages, and provide alternative method to determine whether the overall shift in cell phenotype is primarily driven by VSMC phenotypic modulation rather than changes in other cell populations.

Our study has some limitations that should be addressed to improve the robustness and applicability of the findings. While the use of 4-OHT to modulate progerin expression and prolonged passaging is useful for delineating phenotypic changes, it may not fully capture the complete progression of aging. Alternative methods such as that more closely mimic real biological aging could provide a more comprehensive understanding of VSMC aging behavior.

The key advantage of our approach is that, in vivo, it is challenging to separate healthy/young and pathological/aged cells and their environments, making it difficult to study their interactions. However, in our in vitro model, we can independently recreate healthy/young and pathological/aged arterial conditions, and pair them with VSMCs that are also either healthy/young or pathological/aged. This allows us to investigate their

doi:10.6342/NTU202403815

interactions in a controlled setting, providing valuable insights into the mechanistic underpinnings of vascular aging and disease.

doi:10.6342/NTU202403815

References

1. Murray, C.J., et al., *Global, regional, and national disability-adjusted life years (DALYs) for 306 diseases and injuries and healthy life expectancy (HALE) for 188 countries, 1990-2013: quantifying the epidemiological transition.* Lancet, 2015. **386**(10009): p. 2145-91.
2. Lind, L., et al., *Impact of Aging on the Strength of Cardiovascular Risk Factors: A Longitudinal Study Over 40 Years.* J Am Heart Assoc, 2018. **7**(1).
3. Tucker, W.D., Y. Arora, and K. Mahajan, *Anatomy, Blood Vessels*, in *StatPearls*. 2023, StatPearls Publishing: Treasure Island (FL).
4. Cherng, T.W., O. Jackson-Weaver, and N.L. Kanagy, *13.02 - Introduction to Cardiovascular Physiology ☆*, in *Comprehensive Toxicology (Third Edition)*, C.A. McQueen, Editor. 2018, Elsevier: Oxford. p. 29-45.
5. Wang, D., et al., *Artificial small-diameter blood vessels: materials, fabrication, surface modification, mechanical properties, and bioactive functionalities.* J Mater Chem B, 2020. **8**(9): p. 1801-1822.
6. Gao, Y. *Architecture of the Blood Vessels*. 2017.
7. da Silva, F.C. and C.R. Fürstenau, *Vascular Inflammation: From Cellular Mechanisms to Biotechnology Advances*, in *Biotechnology Applied to Inflammatory Diseases: Cellular Mechanisms and Nanomedicine*. 2023, Springer. p. 19-34.
8. Fung, Y.-c., *Biomechanics: mechanical properties of living tissues*. 2013: Springer Science & Business Media.
9. Brooke, B.S., A. Bayes-Genis, and D.Y. Li, *New Insights into Elastin and Vascular Disease.* Trends in Cardiovascular Medicine, 2003. **13**(5): p. 176-181.
10. Yu, X., et al., *Micromechanics of elastic lamellae: unravelling the role of structural inhomogeneity in multi-scale arterial mechanics.* 2018. **15**(147): p. 20180492.
11. Rodgers, J.L., et al., *Cardiovascular Risks Associated with Gender and Aging.* J Cardiovasc Dev Dis, 2019. **6**(2).
12. Cao, G., et al., *How vascular smooth muscle cell phenotype switching contributes to vascular disease.* Cell Communication and Signaling, 2022. **20**(1): p. 180.
13. van der Linden, J., et al., *Model Systems to Study the Mechanism of Vascular Aging.* Int J Mol Sci, 2023. **24**(20).
14. Zha, Y., et al., *Senescence in Vascular Smooth Muscle Cells and Atherosclerosis.* Front Cardiovasc Med, 2022. **9**: p. 910580.
15. Ataei Ataabadi, E., et al., *Nitric Oxide-cGMP Signaling in Hypertension: Current*

doi:10.6342/NTU202403815

and Future Options for Pharmacotherapy. Hypertension, 2020. **76**(4): p. 1055-1068.
16. Sarkar, R., et al., *Nitric Oxide Reversibly Inhibits the Migration of Cultured Vascular Smooth Muscle Cells.* Circulation Research, 1996. **78**(2): p. 225-230.
17. Gorog, P. and I.B. Kovacs, *Inhibition of Vascular Smooth Muscle Cell Migration by Intact Endothelium Is Nitric Oxide-Mediated: Interference by Oxidised Low Density Lipoproteins.* Journal of Vascular Research, 1998. **35**(3): p. 165-169.
18. van den Oever, I.A.M., et al., *Endothelial Dysfunction, Inflammation, and Apoptosis in Diabetes Mellitus.* Mediators of Inflammation, 2010. **2010**(1): p. 792393.
19. Babici, D., et al., *Mechanisms of increased vascular stiffness down the aortic tree in aging, premenopausal female monkeys.* Am J Physiol Heart Circ Physiol, 2020. **319**(1): p. H222-h234.
20. Wheeler, J.B., et al., *Relation of murine thoracic aortic structural and cellular changes with aging to passive and active mechanical properties.* J Am Heart Assoc, 2015. **4**(3): p. e001744.
21. Taviani, V., et al., *Age-related changes of regional pulse wave velocity in the descending aorta using Fourier velocity encoded M-mode.* Magn Reson Med, 2011. **65**(1): p. 261-8.
22. Astrand, H., et al., *In vivo estimation of the contribution of elastin and collagen to the mechanical properties in the human abdominal aorta: effect of age and sex.* J Appl Physiol (1985), 2011. **110**(1): p. 176-87.
23. Ning, Z., et al., *Vascular Smooth Muscle Cell*, in *Muscle Cell and Tissue*, S. Kunihiro, Editor. 2018, IntechOpen: Rijeka. p. Ch. 11.
24. Metz, R.P., J.L. Patterson, and E. Wilson, *Vascular Smooth Muscle Cells: Isolation, Culture, and Characterization*, in *Cardiovascular Development: Methods and Protocols*, X. Peng and M. Antonyak, Editors. 2012, Humana Press: Totowa, NJ. p. 169-176.
25. Hu, Y., et al., *Abundant progenitor cells in the adventitia contribute to atherosclerosis of vein grafts in ApoE-deficient mice.* The Journal of clinical investigation, 2004. **113**(9): p. 1258-1265.
26. Clément, M., et al., *Vascular smooth muscle cell plasticity and autophagy in dissecting aortic aneurysms.* Arteriosclerosis, thrombosis, and vascular biology, 2019. **39**(6): p. 1149-1159.
27. Brown, I.A.M., et al., *Vascular Smooth Muscle Remodeling in Conductive and Resistance Arteries in Hypertension.* Arteriosclerosis, thrombosis, and vascular biology, 2018. **38**(9): p. 1969-1985.
28. Majesky, M.W., et al., *The adventitia: a dynamic interface containing resident progenitor cells.* Arteriosclerosis, thrombosis, and vascular biology, 2011. **31**(7): p.

doi:10.6342/NTU202403815

1530-1539.
29. Sorokin, V., et al., *Role of Vascular Smooth Muscle Cell Plasticity and Interactions in Vessel Wall Inflammation.* Frontiers in Immunology, 2020. **11**.
30. Frismantiene, A., et al., *Smooth muscle cell-driven vascular diseases and molecular mechanisms of VSMC plasticity.* Cellular Signalling, 2018. **52**: p. 48-64.
31. Salvador, J. and M.L. Iruela-Arispe *Nuclear Mechanosensation and Mechanotransduction in Vascular Cells*. Frontiers in cell and developmental biology, 2022. **10**, 905927 DOI: 10.3389/fcell.2022.905927.
32. Sazonova, O.V., et al., *Extracellular matrix presentation modulates vascular smooth muscle cell mechanotransduction.* Matrix Biology, 2015. **41**: p. 36-43.
33. Stegemann, J.P., H. Hong, and R.M. Nerem, *Mechanical, biochemical, and extracellular matrix effects on vascular smooth muscle cell phenotype.* 2005. **98**(6): p. 2321-2327.
34. Vatankhah, E., et al., *Phenotypic modulation of smooth muscle cells by chemical and mechanical cues of electrospun tecophilic/gelatin nanofibers.* ACS Appl Mater Interfaces, 2014. **6**(6): p. 4089-101.
35. Xie, S.-A., et al., *Matrix stiffness determines the phenotype of vascular smooth muscle cell in vitro and in vivo: Role of DNA methyltransferase 1.* Biomaterials, 2018. **155**: p. 203-216.
36. Varga, R., et al., *Progressive vascular smooth muscle cell defects in a mouse model of Hutchinson–Gilford progeria syndrome.* Proceedings of the National Academy of Sciences, 2006. **103**(9): p. 3250-3255.
37. Hamczyk, M.R., et al., *Vascular smooth muscle–specific progerin expression accelerates atherosclerosis and death in a mouse model of Hutchinson-Gilford progeria syndrome.* Circulation, 2018. **138**(3): p. 266-282.
38. Coll-Bonfill, N., et al., *Progerin induces a phenotypic switch in vascular smooth muscle cells and triggers replication stress and an aging-associated secretory signature.* GeroScience, 2022.
39. Xu, S. and Z.-G. Jin, *Hutchinson–Gilford Progeria Syndrome: Cardiovascular Pathologies and Potential Therapies.* Trends in Biochemical Sciences, 2019. **44**(7): p. 561-564.
40. Olive, M., et al., *Cardiovascular pathology in Hutchinson-Gilford progeria: correlation with the vascular pathology of aging.* Arterioscler Thromb Vasc Biol, 2010. **30**(11): p. 2301-9.
41. Ragnauth, C.D., et al., *Prelamin A acts to accelerate smooth muscle cell senescence and is a novel biomarker of human vascular aging.* Circulation, 2010. **121**(20): p. 2200-2210.

doi:10.6342/NTU202403815

42. Scaffidi, P. and T. Misteli, *Lamin A-dependent nuclear defects in human aging.* Science, 2006. **312**(5776): p. 1059-1063.
43. Jensen, L.F., J.F. Bentzon, and J. Albarrán-Juárez, *The Phenotypic Responses of Vascular Smooth Muscle Cells Exposed to Mechanical Cues.* Cells, 2021. **10**(9): p. 2209.
44. Hahn, C. and M.A. Schwartz, *Mechanotransduction in vascular physiology and atherogenesis.* Nature reviews Molecular cell biology, 2009. **10**(1): p. 53-62.
45. Osman, O.S., et al., *A novel method to assess collagen architecture in skin.* BMC Bioinformatics, 2013. **14**(1): p. 260.
46. Yamashiro, Y. and H. Yanagisawa, *The molecular mechanism of mechanotransduction in vascular homeostasis and disease.* Clin Sci (Lond), 2020. **134**(17): p. 2399-2418.
47. Lee, H.Y. and B.H. Oh, *Aging and arterial stiffness.* Circ J, 2010. **74**(11): p. 2257-62.
48. Benedicto, I., B. Dorado, and V. Andrés, *Molecular and Cellular Mechanisms Driving Cardiovascular Disease in Hutchinson-Gilford Progeria Syndrome: Lessons Learned from Animal Models.* Cells, 2021. **10**(5).
49. Mammoto, A., K. Matus, and T. Mammoto, *Extracellular Matrix in Aging Aorta.* Front Cell Dev Biol, 2022. **10**: p. 822561.
50. Castelli, R., et al., *Aging of the Arterial System.* International Journal of Molecular Sciences, 2023. **24**(8): p. 6910.
51. Liu, S. and Z. Lin, *Vascular Smooth Muscle Cells Mechanosensitive Regulators and Vascular Remodeling.* J Vasc Res, 2022. **59**(2): p. 90-113.
52. Qiu, J., et al., *Biomechanical regulation of vascular smooth muscle cell functions: from in vitro to in vivo understanding.* J R Soc Interface, 2014. **11**(90): p. 20130852.
53. Guan, X., et al., *Stress, Vascular Smooth Muscle Cell Phenotype and Atherosclerosis: Novel Insight into Smooth Muscle Cell Phenotypic Transition in Atherosclerosis.* Curr Atheroscler Rep, 2024. **26**(8): p. 411-425.
54. Bajpai, A., R. Li, and W. Chen, *The cellular mechanobiology of aging: from biology to mechanics.* Ann N Y Acad Sci, 2021. **1491**(1): p. 3-24.
55. Brozovich, F.V., et al., *Mechanisms of Vascular Smooth Muscle Contraction and the Basis for Pharmacologic Treatment of Smooth Muscle Disorders.* Pharmacol Rev, 2016. **68**(2): p. 476-532.
56. Wang, W.P., et al., *Progerin in muscle leads to thermogenic and metabolic defects via impaired calcium homeostasis.* Aging Cell, 2020. **19**(2): p. e13090.
57. Wen, S.-M., W.-C. Wen, and P.-h.G. Chao, *Zyxin and actin structure confer anisotropic YAP mechanotransduction.* Acta Biomaterialia, 2022. **152**: p. 313-320.

doi:10.6342/NTU202403815

58. Vatner, S.F., et al., *Vascular Stiffness in Aging and Disease.* Frontiers in Physiology, 2021. **12**.
59. Qiu, H., et al., *Mechanism of gender-specific differences in aortic stiffness with aging in nonhuman primates.* Circulation, 2007. **116**(6): p. 669-76.
60. Qiu, H., et al., *Short communication: vascular smooth muscle cell stiffness as a mechanism for increased aortic stiffness with aging.* Circ Res, 2010. **107**(5): p. 615-9.
61. Birch, H.L., *Extracellular Matrix and Ageing.* Subcell Biochem, 2018. **90**: p. 169-190.
62. Halka, A.T., et al., *The effects of stretch on vascular smooth muscle cell phenotype in vitro.* Cardiovasc Pathol, 2008. **17**(2): p. 98-102.
63. Mantella, L.E., A. Quan, and S. Verma, *Variability in vascular smooth muscle cell stretch-induced responses in 2D culture.* Vasc Cell, 2015. **7**: p. 7.
64. Zhang, M.-J., et al., *An overview of potential molecular mechanisms involved in VSMC phenotypic modulation.* Histochemistry and Cell Biology, 2016. **145**(2): p. 119-130.
65. Rensen, S.S.M., P.A.F.M. Doevendans, and G.J.J.M. van Eys, *Regulation and characteristics of vascular smooth muscle cell phenotypic diversity.* Netherlands Heart Journal, 2007. **15**(3): p. 100-108.
66. Farina, F.M., et al., *miR-128-3p Is a Novel Regulator of Vascular Smooth Muscle Cell Phenotypic Switch and Vascular Diseases.* Circ Res, 2020. **126**(12): p. e120-e135.
67. Xin, Y., et al., *Elucidating VSMC phenotypic transition mechanisms to bridge insights into cardiovascular disease implications.* Frontiers in Cardiovascular Medicine, 2024. **11**.
68. Hamczyk, M.R. and R.M. Nevado, *Vascular smooth muscle cell aging: Insights from Hutchinson-Gilford progeria syndrome.* Clin Investig Arterioscler, 2023. **35**(1): p. 42-51.
69. Del Campo, L., et al., *Vascular Smooth Muscle Cell-Specific Progerin Expression Provokes Contractile Impairment in a Mouse Model of Hutchinson-Gilford Progeria Syndrome that Is Ameliorated by Nitrite Treatment.* Cells, 2020. **9**(3).
70. Dobnikar, L., et al., *Disease-relevant transcriptional signatures identified in individual smooth muscle cells from healthy mouse vessels.* Nat Commun, 2018. **9**(1): p. 4567.
71. Zhao, Y., et al., *Osteopontin/SPP1: a potential mediator between immune cells and vascular calcification.* Front Immunol, 2024. **15**: p. 1395596.
72. Ashraf, J.V. and A. Al Haj Zen, *Role of Vascular Smooth Muscle Cell Phenotype*

doi:10.6342/NTU202403815

Switching in Arteriogenesis. International Journal of Molecular Sciences, 2021. **22**(19): p. 10585.

73. Huang, K., et al., *SIRT1 and FOXO Mediate Contractile Differentiation of Vascular Smooth Muscle Cells under Cyclic Stretch.* Cellular Physiology and Biochemistry, 2015. **37**(5): p. 1817-1829.
74. Yao, Q.-P., et al., *The role of SIRT6 in the differentiation of vascular smooth muscle cells in response to cyclic strain.* The International Journal of Biochemistry & Cell Biology, 2014. **49**: p. 98-104.
75. Mao, X., et al., *Cyclic stretch-induced thrombin generation by rat vascular smooth muscle cells is mediated by the integrin αvβ3 pathway.* Cardiovascular Research, 2012. **96**(3): p. 513-523.
76. Yap, C., et al., *Six Shades of Vascular Smooth Muscle Cells Illuminated by KLF4 (Krüppel-Like Factor 4).* Arteriosclerosis, Thrombosis, and Vascular Biology, 2021. **41**(11): p. 2693-2707.
77. Zhang, Y., et al., *Krüppel-like factors in tumors: Key regulators and therapeutic avenues.* Frontiers in Oncology, 2023. **13**: p. 1080720.
78. Xie, Z., et al., *Current knowledge of Krüppel-like factor 5 and vascular remodeling: providing insights for therapeutic strategies.* Journal of Molecular Cell Biology, 2021. **13**(2): p. 79-90.
79. Rodríguez, A.I., et al., *MEF2B-Nox1 Signaling Is Critical for Stretch-Induced Phenotypic Modulation of Vascular Smooth Muscle Cells.* Arteriosclerosis, Thrombosis, and Vascular Biology, 2015. **35**(2): p. 430-438.
80. Philip, J.T. and K.N. Dahl, *Nuclear mechanotransduction: response of the lamina to extracellular stress with implications in aging.* J Biomech, 2008. **41**(15): p. 3164-70.
81. Swift, J., et al., *Nuclear lamin-A scales with tissue stiffness and enhances matrix-directed differentiation.* Science, 2013. **341**(6149): p. 1240104.
82. Song, M., et al., *Shear stress-induced mechanotransduction protein deregulation and vasculopathy in a mouse model of progeria.* Stem Cell Research & Therapy, 2014. **5**(2): p. 41.
83. Brassard, J.A., et al., *Hutchinson-Gilford progeria syndrome as a model for vascular aging.* Biogerontology, 2016. **17**(1): p. 129-45.
84. Chang, W., et al., *Imbalanced nucleocytoskeletal connections create common polarity defects in progeria and physiological aging.* Proceedings of the National Academy of Sciences, 2019. **116**(9): p. 3578-3583.
85. Chen, Z.J., et al., *Dysregulated interactions between lamin A and SUN1 induce abnormalities in the nuclear envelope and endoplasmic reticulum in progeric laminopathies.* J Cell Sci, 2014. **127**(Pt 8): p. 1792-804.

doi:10.6342/NTU202403815

86. Booth, E.A., et al., *Nuclear stiffening and chromatin softening with progerin expression leads to an attenuated nuclear response to force.* Soft Matter, 2015. **11**(32): p. 6412-8.
87. Przybylska, D., et al., *NOX4 downregulation leads to senescence of human vascular smooth muscle cells.* Oncotarget, 2016. **7**(41): p. 66429-66443.
88. Wang, Z., D. Wei, and H. Xiao, *Methods of cellular senescence induction using oxidative stress.* Methods Mol Biol, 2013. **1048**: p. 135-44.
89. Tripathi, M., P.M. Yen, and B.K. Singh, *Protocol to Generate Senescent Cells from the Mouse Hepatic Cell Line AML12 to Study Hepatic Aging.* STAR Protoc, 2020. **1**(2): p. 100064.
90. Prowse, K.R. and C.W. Greider, *Developmental and tissue-specific regulation of mouse telomerase and telomere length.* Proceedings of the National Academy of Sciences, 1995. **92**(11): p. 4818-4822.
91. Nan-PIng, W. and R.J. Hodes, *The role of telomerase expression and telomere length maintenance in human and mouse.* Journal of clinical immunology, 2000. **20**: p. 257-267.
92. Blasco, M.A., *Telomere length, stem cells and aging.* Nature chemical biology, 2007. **3**(10): p. 640-649.
93. Hu, X. and H. Zhang, *Doxorubicin-Induced Cancer Cell Senescence Shows a Time Delay Effect and Is Inhibited by Epithelial-Mesenchymal Transition (EMT).* Med Sci Monit, 2019. **25**: p. 3617-3623.
94. Bientinesi, E., et al., *Doxorubicin-induced senescence in normal fibroblasts promotes in vitro tumour cell growth and invasiveness: The role of Quercetin in modulating these processes.* Mech Ageing Dev, 2022. **206**: p. 111689.
95. Elmarasi, M., et al., *Phenotypic switching of vascular smooth muscle cells in atherosclerosis, hypertension, and aortic dissection.* J Cell Physiol, 2024. **239**(4): p. e31200.
96. Jiang, Y. and H.-Y. Qian, *Transcription factors: Key regulatory targets of vascular smooth muscle cell in atherosclerosis.* Molecular Medicine, 2023. **29**(1): p. 2.
97. Chang, W., et al., *Isolation and Cultivation of Vascular Smooth Muscle Cells from the Mouse Circle of Willis.* J Vasc Res, 2023. **60**(4): p. 234-244.

doi:10.6342/NTU202403815

Appendix

Table 1 PCR primer

Gene	Primer sequence	NCBI Ref Seq
Housekeeping gene		
GAPDH	F: CTGCACCACCACCAACTGCTTAG R: GGGCCATCCACAGTCTTCT	NM_001289726.1
Contractile genes		
Acta2	F: AGAGCAAGAGAGGGATCCTGA R: GTCGTCCCAGTTGGTGATGAT	NM_007392.3
Taglin	F: TGAAGAAAGCCCAGGAGCAT R: TGCTTCCCCTCCTGCAGTT	NM_011526.5
Myh11	F: GCAATGCGAAAACCGTCAA R: GATGCGAATGAACTTGCCAAA	NM_013607.2
Cnn1	F: TCTGCACATTTTAAACCGAGGTG R: GCCAGCTTGTTCTTTACTTCAGC	XM_011242388.3
Synthetic genes		
Spp1	F: AGCAAGAAACTCTTCCAAGCAA R: GTGAGATTCGTCAGATTCATCCG	NM_001204201.1
Klf5	F: CGATTCACAACCCAAATTTACC R: GTATGAGTCCTCAGGTGAGCTTTTA	NM_009769.4
Col1a1	F: AGAGCATGACCGATGGATTC R: AGGCCTCGGTGGACATTAG	NM_007742.4

doi:10.6342/NTU202403815

Table 2 Antibody

Primary antibody

Target	Host	Dilution	Clone	Product number
α-smooth muscle actin	mouse	1:500	Monoclonal	Sigma #A2547
SM-22 (transgelin)	rabbit	1:500	Polyclonal	Abcam #ab14106
Calponin-1	rabbit	1:250	Monoclonal	Abcam #ab46794
FLAG	mouse	1:1200	Polyclonal	Cell Signaling #2368S

Secondary antibody

Target	Product number
Alexa Fluor 488 anti-mouse IgG	Invitrogen #A-11001
Alexa Fluor 647 anti-rabbit IgG	Invitrogen #A-21245

doi:10.6342/NTU202403815